

Scaling of bipartite entanglement in one-dimensional lattice systems with a trapping potential

Massimo Campostrini and Ettore Vicari

Dipartimento di Fisica dell'Università di Pisa and INFN, Sezione di Pisa, Largo
Bruno Pontecorvo 2, I-56127 Pisa, Italy

Abstract.

We study the effects of a power-law trapping potential on the scaling behaviour of the entanglement at the quantum critical point of one-dimensional (1D) lattice particle systems. We compute bipartite von Neumann and Rényi entropies in the presence of the trap, and analyze their scaling behaviour with increasing the trap size.

As a theoretical laboratory, we consider the quantum XY chain in an external transverse field acting as a trap for the spinless fermions of its quadratic Hamiltonian representation. We then investigate confined particle systems described by the 1D Bose-Hubbard model in the superfluid phase (around the center of the trap).

In both cases conformal field theory predicts logarithmically divergent bipartite entanglement entropies for the homogeneous systems without trap. The presence of the trapping potential breaks conformal invariance, affecting the critical behaviour of the homogeneous system. Our results show that the bipartite entanglement entropies diverge logarithmically with increasing the trap size, and present notable scaling behaviours in the trap-size scaling limit.

1. Introduction

The spatial entanglement of one-dimensional (1D) lattice systems near their quantum critical point is a physical issue which has attracted much interest, see, e.g., Ref. [1]. Many studies have been devoted to quantify it, by computing von Neumann or Rényi entanglement entropies of the reduced density matrix of a subsystem. In a homogeneous system of length L whose quantum critical behaviour is described by a two-dimensional (2D) conformal field theory (CFT), the bipartite entanglement entropy $S(l_A, L)$ increases logarithmically [2, 3, 4, 5] with increasing the size l_A of the subsystem at the critical point, i.e., $S \sim \ln l_A$, or with increasing the spatial length scale ξ when approaching the critical point, i.e., $S \sim \ln \xi$ (if $1 \ll \xi \ll l_A$). In both cases the coefficients of the logarithms are related to the central charge of the corresponding CFT.

Quantum lattice particle systems are realized in experiments of cold atoms in optical lattices of any effective spatial dimension $d \leq 3$, which allow to investigate the interesting interplay between quantum and statistical behaviours in particle systems, see, e.g., Refs. [6, 7, 8, 9, 10, 11, 12, 13, 14, 15, 16, 17]. An important feature of these experiments is the presence of a confining potential which traps the particles within

a limited spatial region of the optical lattice created by laser-induced standing waves. The theoretical framework [18] is based on the Bose-Hubbard (BH) model [19] in the presence of a confining potential coupled to the particle density, i.e.,

$$H_{\text{BH}} = -\frac{J}{2} \sum_{\langle ij \rangle} (b_i^\dagger b_j + b_j^\dagger b_i) + \frac{U}{2} \sum_i n_i(n_i - 1) + \mu \sum_i n_i + \sum_i V(r_i) n_i, \quad (1)$$

where $\langle ij \rangle$ is the set of nearest-neighbour sites, $n_i \equiv b_i^\dagger b_i$ is the particle density operator. We consider a power-law trapping potential

$$V(r) = v^p r^p \equiv (r/l)^p, \quad (2)$$

where $r \equiv |\vec{x}|$, v and p are positive constants and $l \equiv 1/v$ is the trap size. Experiments are usually set up with a harmonic potential, i.e., $p = 2$. Far from the origin the potential $V(r)$ diverges, therefore $\langle n_i \rangle$ vanishes and the particles are trapped. The inhomogeneity due to the trapping potential strongly affects the phenomenology of quantum transitions in homogeneous systems. The correlation functions develop critical behaviours only in the limit of large trap size. This critical behaviour can be described in the framework of the trap-size scaling (TSS) theory [20, 21].

In this paper we focus on the quantum entanglement in lattice particle systems confined by an external potential, such as the BH model (1). We investigate how the scaling behaviour of the entanglement entropies determined by CFT changes in the presence of the inhomogeneity induced by the confining potential.

As a theoretical laboratory we consider the quantum XY chain in an external space-dependent transverse field, acting as a trap for the spinless fermions of its quadratic Hamiltonian representation. This model presents a quantum critical behaviour belonging to the 2D Ising universality class, thus described by a CFT with central charge $c = 1/2$. In the presence of the trap and for large trap sizes, the quantum critical behaviour shows TSS [20, 21]. The presence of the trap induces a length scale ξ at the critical point, which scales nontrivially with increasing the trap size, i.e., as $\xi \sim l^\theta$ with a trap exponent $\theta = p/(p + 1)$.

We then consider the 1D BH model (1) in its hard-core limit, i.e., $U \rightarrow \infty$, and study the bipartite entanglement entropy in the gapless superfluid phase, whose continuum limit is described by a 2D massless bosonic field theory, thus a CFT with $c = 1$. In this case the trap-size dependence is made more complicated by new features [22]: (i) a multiscaling phenomenon, i.e., the existence of different length scales which diverge with distinct power laws in the TSS; (ii) the presence of level crossings of the lowest states at finite trap size, which gives rise to a peculiar modulation of the amplitudes of the asymptotic power-law behaviours.

We analyze the scaling behaviour of bipartite von Neumann and Rényi entanglement entropies in these 1D lattice models. We consider chains with even sites L and open boundary conditions, and a trap of size l centered between the middle sites of the chain. We divide the chain in two connected parts of length l_A and $L - l_A$, and consider their von Neumann entropy

$$S_1(l_A; L) = S_1(L - l_A; L) = -\text{Tr}[\rho_A \ln \rho_A] \quad (3)$$

and their Rényi entropies

$$S_\alpha(l_A; L) = S_\alpha(L - l_A; L) = \frac{1}{1 - \alpha} \ln \text{Tr} \rho_A^\alpha \quad (4)$$

where ρ_A is the reduced density matrix of one of the two subsystems. Rényi entropies are useful because they provide information on the spectrum of ρ_A [23]. The von Neumann entropy (3) is obtained by taking the limit $\alpha \rightarrow 1$ in (4). In the presence of a trap of size l , the bipartite entanglement entropies of subsystems of size $l_A = L/2 - x$ have a finite $L \rightarrow \infty$ limit, depending on x and l . We study their scaling behaviour in the large- l limit. Note that the $p \rightarrow \infty$ limit of the confining potential becomes equivalent to a homogeneous chain of size $L = 2l$ with open boundary conditions (more precisely, to a chain with even $L = 2[l]$ sites). Thus, in the $p \rightarrow \infty$ limit we must recover the entanglement entropies of homogeneous systems with open boundary conditions, which are determined by CFT.

In our numerical study we exploit the quadratic spinless fermion representations of the XY chain and the 1D hard-core BH model, which allow us to perform computations for very large systems, since they only require the diagonalization of a $L \times L$ matrix where L is the number of lattice sites. We compute the entanglement entropies using the method outlined in Refs. [24, 25], which exploits the quadratic fermionic representation and can be also applied in the presence of the trapping potential. We obtain numerical results for chains of size L and open boundary conditions, with a trap of size l centered between the middle sites of the chain; we choose L large enough to have negligible finite- L effects; we are able to obtain very accurate results for l up to $O(10^4)$.

Our results show that the bipartite entanglement entropies at the critical point diverge logarithmically with increasing the trap size. Moreover, they present notable scaling behaviours in the trap-size scaling limit.

We mention that the bipartite entanglement entropies in the XY and XX model with gradients, i.e., in the presence of a linear external field, have been recently investigated in Ref. [26].

The paper is organized as follows. In Sec. 2 we presents results for the quantum XY chain in an external space-dependent transverse field. Sec. 3 is dedicated to the 1D hard-core BH model. In Sec. 4 we draw our conclusions.

2. Bipartite entanglement in the XY chain with a space-dependent transverse field

The quantum XY chain in a transverse field is a standard theoretical laboratory for issues related to quantum transitions, see, e.g., Ref. [27]. An inhomogeneity analogous to the one arising from a trapping potential in particle systems can be achieved by considering a space-dependent transverse field, i.e.,

$$H_{\text{XY}} = - \sum_i \frac{1}{2} [(1 + \gamma) \sigma_i^x \sigma_{i+1}^x + (1 - \gamma) \sigma_i^y \sigma_{i+1}^y] - \mu \sigma_i^z - V(x_i) \sigma_i^z, \quad (5)$$

where σ^i are the Pauli matrices, $\gamma \neq 0$ and $V(x) = (|x|/l)^p$, cf. (2). The XY chain can be mapped into a quadratic Hamiltonian of spinless fermions by a Jordan-Wigner transformation, obtaining

$$\begin{aligned} H &= \sum [c_i^\dagger A_{ij} c_j + \frac{1}{2}(c_i^\dagger B_{ij} c_j^\dagger + \text{h.c.})], \\ A_{ij} &= 2\delta_{ij} - \delta_{i+1,j} - \delta_{i,j+1} + 2Q(x_i)\delta_{ij}, \\ B_{ij} &= -\gamma(\delta_{i+1,j} - \delta_{i,j+1}), \\ Q(x) &= \bar{\mu} + V(x), \quad \bar{\mu} \equiv \mu - 1. \end{aligned} \tag{6}$$

In this picture μ plays the role of *chemical potential* for the fermion *c-particles*, and the space-dependent field $V(x)$ acts as a *trap* for the *c-particles*, making their *local density* $\langle n_i \rangle \equiv \langle c_i^\dagger c_i \rangle$ vanish at large distance. In the following, l will be considered as the *trap size*.

In the absence of the trap, the model undergoes a quantum transition at $\bar{\mu} \equiv \mu - 1 = 0$ in the 2D Ising universality class, separating a quantum paramagnetic phase for $\bar{\mu} > 0$ from a quantum ferromagnetic phase for $\bar{\mu} < 0$. Around $\bar{\mu} = 0$, the quantum critical behaviour shows a diverging length scale, $\xi \sim |\bar{\mu}|^{-\nu}$, and a vanishing energy scale, $\Delta \sim \xi^{-z}$, where z and ν are universal critical exponents: $z = 1$ and $\nu \equiv 1/y_\mu = 1$ (y_μ is the RG dimension of μ).

The presence of the external field $V(x)$ gives rise to a space inhomogeneity, thus affecting the critical behaviour of the homogeneous system, which is only recovered in the limit of large trap size. In this limit the critical behaviour can be described in the framework of the trap-size scaling (TSS) theory [20]. The TSS Ansatz for the asymptotic behaviour of the free-energy density in the presence of a confining potential (2) is

$$F(\mu, T, l, x) = l^{-\theta(1+z)} \mathcal{F}(\bar{\mu} l^{\theta/\nu}, T l^{\theta z}, x l^{-\theta}), \tag{7}$$

where x is the distance from the middle of the trap, and θ is the trap-size exponent which determines how the length scale of the critical modes at the critical point diverges with increasing trap size, i.e., $\xi \sim l^\theta$. RG arguments and analytic calculations show that [20]

$$\theta = p/(p+1). \tag{8}$$

The TSS limit can be analytically derived within the quadratic spinless fermion representation (6), obtaining a Schrödinger-like equation for the lowest states, after introducing the rescaled spatial variable $X \equiv \gamma^{-\theta/p} l^{-\theta} x$, and the rescaled deviation from the critical point $\mu_r \equiv \gamma^{-\theta} l^\theta \bar{\mu}$ (see Ref. [20] for details). The γ dependence gets absorbed by such rescalings leading to a universal TSS limit. Therefore at the quantum critical point $\bar{\mu} = 0$ and $T = 0$, any length scale related to the critical modes must have the asymptotic behaviour

$$\xi = a \gamma^{\theta/p} l^\theta [1 + O(l^{-\theta})] \tag{9}$$

where the amplitude a depends on the power p of the potential, but not on γ . The power law of the scaling corrections is inferred from the analysis of the corrections to the continuum Schrödinger-like equation describing the TSS limit.

We want to study the quantum entanglement of the ground-state in the presence of the external space-dependent potential (2). For this purpose we analyze the trap-size dependence of the bipartite von Neumann and Rényi entanglement entropies, defined in equations (3) and (4), in the framework of the TSS theory.

Before presenting the results in the presence of the trap, let us recall some established results for the homogeneous XY chain with open boundary conditions, which represents the formal $p \rightarrow \infty$ limit of the model with the confining potential. They can be obtained by exploiting the CFT that describes its continuum limit. Setting

$$l_A = L/2 - x \quad (10)$$

(we consider a chain with an even number of sites L), the Rényi entropies at the critical point $\bar{\mu} = 0$ behave as [4]

$$S_\alpha(L/2 - x; L) \approx C_\alpha \left[\ln L + \ln \cos \left(\frac{\pi x}{L} \right) + e_\alpha \right] \quad (11)$$

where

$$C_\alpha \equiv c \frac{1 + \alpha^{-1}}{12} \quad (12)$$

and c is the central charge: $c = 1/2$ for the 2D Ising universality class. The constant e_α can be derived using the results of Refs. [4, 28, 29, 20], obtaining

$$e_\alpha = \ln \gamma + \ln(8/\pi) + y_\alpha, \quad (13)$$

$$y_\alpha = \int_0^\infty \frac{dt}{t} \left[\frac{6}{1 - \alpha^{-2}} \left(\frac{1}{\alpha \sinh t/\alpha} - \frac{1}{\sinh t} \right) \frac{1}{\sinh t} - e^{-2t} \right].$$

The behaviour of the von Neumann entropy can be obtained by taking the limit $\alpha \rightarrow 1$ of (11). Corrections to the asymptotic behaviour (11) are expected to be $O(L^{-1/\alpha})$ at fixed x/L [30, 31]. They become logarithmic for $\alpha \rightarrow \infty$. In the case of the von Neumann entropy, i.e., $\alpha \rightarrow 1$, corrections are $O(L^{-1})$.[‡]

In the presence of the trap of size l , the dependence on L rapidly disappears for L sufficiently larger than the trap size l . We define entanglement length scales ξ_α from the half-lattice entanglement entropies. We write (at $\bar{\mu} = 0$)

$$S_{\alpha,1/2} \equiv \lim_{L \rightarrow \infty} S_\alpha(L/2; L) \equiv C_\alpha (\ln \xi_\alpha + e_\alpha), \quad (14)$$

where e_α is the constant defined in (13). We identify the argument of the logarithm as the entanglement length scale ξ_α , which will generally depend on α and on the power p of the potential (2). However, by construction, their $p \rightarrow \infty$ limit is $\xi_\alpha \rightarrow 2l = L$ for any α . Since the entanglement length scales are clearly related to the critical modes, they are expected to have the asymptotic behaviour (9) at the critical point, although their scaling corrections may turn out to be different, depending on α .

The approach to their asymptotic behaviour $\xi_\alpha \sim l^\theta$ may be guessed by recalling that the $p \rightarrow \infty$ limit is equivalent to a homogeneous chain of size $L = 2l$ with open boundary conditions, where the corrections to the asymptotic behaviour (11) of the

[‡] It is worth mentioning that, using the relation [29] $S_\alpha(l_A; L)|_{\gamma=1} = \frac{1}{2} S_\alpha(2l_A; 2L)|_{\gamma=0}$ and results from Refs. [32, 22], we obtain $S_1(L/2; L) = \frac{1}{12} [\ln L + e_1 + (2 - 3\pi)/(4L) + O(1/L^2)]$ for $\gamma = 1$.

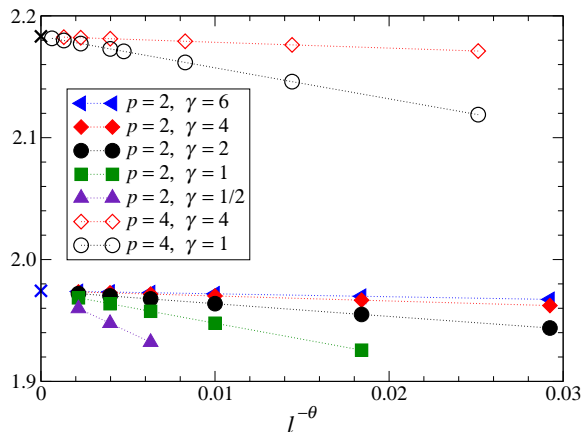


Figure 1. The ratio $\xi_1/(\gamma^{\theta/p}l^\theta)$ vs $l^{-\theta}$ for $p = 2, 4$, several values of γ , and trap sizes in the range $10^2 \leq l \leq 10^4$. The lines are drawn to guide the eyes. The crosses along the y -axis represent the γ -independent $l \rightarrow \infty$ extrapolations, see text.

Rényi entanglement entropies are [31] $O(L^{-1/\alpha})$. Then, the correspondence $L \rightarrow \xi \sim l^\theta$ suggests the presence of $O(\xi^{-1/\alpha})$, thus $O(l^{-\theta/\alpha})$, corrections. In the case of the length scale derived from the von Neumann entropy, i.e., for $\alpha \rightarrow 1$, this argument leads to the same scaling corrections of equation (9), which are expected for any length scale defined from standard correlation functions, such as $G_{ij} \equiv \langle \sigma_i^x \sigma_j^x \rangle$.

The scaling (9) is fully supported by numerical results for the half-lattice von Neumann entropy. § Figure 1 shows the results of ξ_1 for $p = 2$ and $p = 4$, several values of γ , and for trap sizes in the range $10^2 \leq l \leq 10^4$. In order to estimate the amplitude a_1 of the asymptotic behaviour

$$\xi_1 = a_1 \gamma^{\theta/p} l^\theta [1 + b_{11} l^{-\theta} + \dots], \quad (15)$$

we fit the data of the ratio $\xi_1/(\gamma^{\theta/p}l^\theta)$ to the Ansatz $a_1 + b_{1,1}l^{-\theta} + b_{1,2}l^{-2\theta}$, which turns out to be optimal, and check the stability of the results by increasing the minimum value of l allowed in the fit. The analysis of the $p = 2$ data gives $a_1 \approx 1.97431$ for all $\gamma = 6, 4, 2, 1, 1/2$,|| confirming its independence of γ , and $b_{1,1} = \bar{b}_{1,1}\gamma^{4/3}$ with $\bar{b}_{11} \approx -2.677$ independent of γ . For $p = 4$ we obtain $a_1 \approx 2.18316$ for both $\gamma = 4, 1$.

In the case of the entanglement length scales ξ_α defined from the Rényi entropies, we generally expect $\xi_\alpha \sim l^\theta$ asymptotically, with $O(l^{-\theta/\alpha})$ corrections. Assuming universality of the TSS limit, we expect that the ratios ξ_α/ξ_1 approach universal values R_α ,

$$\xi_\alpha/\xi_1 = R_\alpha + O(l^{-\theta/\alpha}) \quad (16)$$

§ The effects of the finite size L of the chain are under complete control in our numerical calculations at fixed trap size. This is easily achieved by comparing data at fixed trap size for increasing chain size, due to the fast convergence to the infinite-chain limit, see also later. We choose L large enough to have negligible finite- L effects, so that the results that we present can be effectively considered as infinite-chain results with great accuracy. Therefore, the systematic error related to the finite size of the chain is totally negligible in our analyses.

|| Here and in the following the uncertainty on the numerical estimates is at most one on the last reported figure.

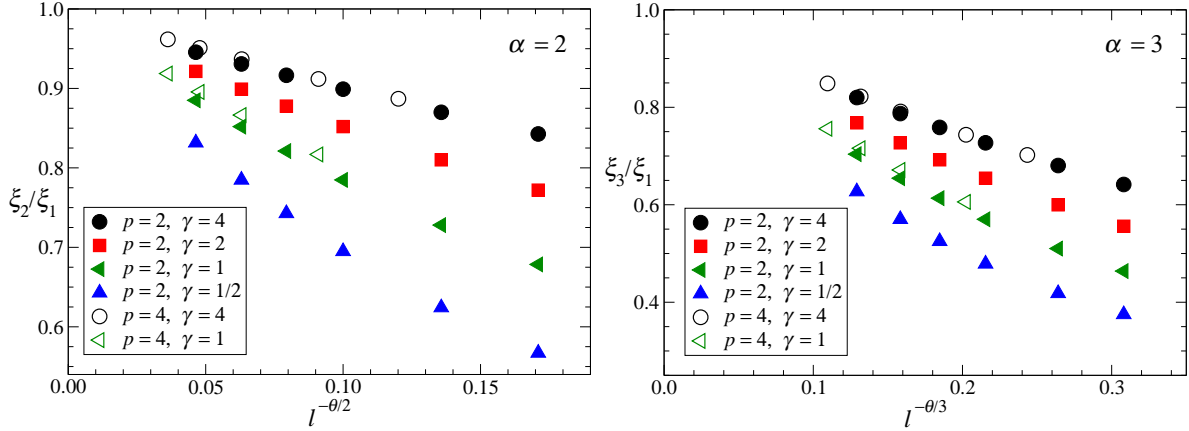


Figure 2. Ratios ξ_α/ξ_1 of entanglement length scales vs. $l^{-\theta/\alpha}$ in the presence of an external potential with $p = 2, 4$, for $\alpha = 2, 3$, several values of γ , and trap sizes in the range $10^2 \leq l \leq 10^4$.

and therefore

$$\xi_\alpha = a_\alpha \gamma^{\theta/p} l^\theta [1 + b_{\alpha,1}(\gamma) l^{-\theta/\alpha} + b_{\alpha,2}(\gamma) l^{-2\theta/\alpha} + \dots], \quad (17)$$

with a_α dependent on p but not on γ . Note that $R_\alpha \rightarrow 1$ and $a_\alpha \rightarrow 2$ for $p \rightarrow \infty$.

This scenario is confirmed by numerical results for the ratios ξ_α/ξ_1 , see figure 2 where we show results for $p = 2, 4$ and $\alpha = 2, 3$. They fit the general behaviour

$$\xi_\alpha/\xi_1 = R_\alpha + \sum_{j=1} c_j l^{-j\theta/\alpha}, \quad (18)$$

and provide consistent values of R_α for different values of γ , supporting universality. For example, we find $R_2 \approx 0.9889$, $R_3 \approx 0.987$ for $p = 2$, and $R_2 \approx 0.9970$ and $R_3 \approx 0.996$ for $p = 4$, which are slightly smaller than one, and appear to approach one with increasing p . ¶

Moreover, the results for $p = 2$ indicate that the amplitudes $b_{\alpha,1}$ of the leading $O(l^{-\theta/\alpha})$ scaling corrections in equation (17) behave as $b_{\alpha,1} = \bar{b}_{\alpha,1} \gamma^{-\kappa/\alpha}$ where $\kappa = 4/3$ and $\bar{b}_{\alpha,1}$ is independent of γ , with great numerical accuracy. Analogous results are found for $p = 4$, but with $\kappa = 6/5$. Taking into account that $b_{\alpha,1} \sim \gamma^{-1/\alpha}$ for $p \rightarrow \infty$ (as inferred by numerical computations), we may guess $\kappa = (p+2)/(p+1)$. Therefore, we have that the ratios $b_{\alpha,1}^\alpha/b_{1,1}$ are independent of γ . Note that this also implies that the leading $O(l^{-\theta/\alpha})$ scaling corrections get suppressed with increasing γ for any α , including $\alpha \rightarrow 1$.

Let us now study the spatial dependence of the entanglement entropy in the presence of the trap. For this purpose we define the function

$$s_\alpha(x) \equiv C_\alpha^{-1} \lim_{L \rightarrow \infty} [S_\alpha(L/2 - x; L) - S_\alpha(L/2; L)] \quad (19)$$

¶ To get an idea of the accuracy of the universality check, we mention that, using the six available data in the range $10^2 \leq l \leq 10^4$ to fix the six parameters of the polynomial $R_\alpha + \sum_{j=1}^5 c_j e^{-j\theta/\alpha}$, we obtain $R_2 = 0.98892, 0.98892, 0.98892, 0.98889$ and $R_3 = 0.9867, 0.9867, 0.9868, 0.9869$ for $\gamma = 4, 2, 1, 1/2$ respectively.

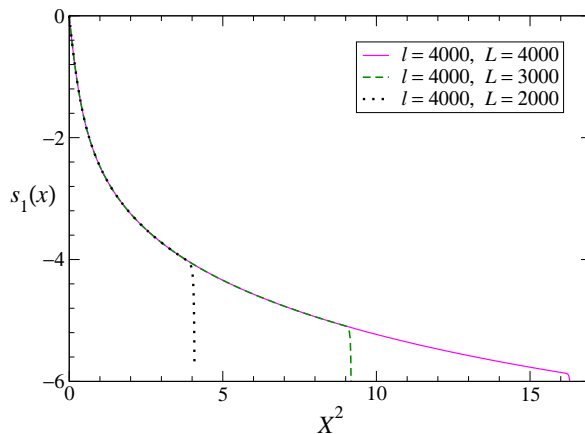


Figure 3. $s_1(x)$, cf. (19), vs. X^2 , for $\gamma = 1$, $p = 2$, $l = 4000$ and a few values of the size of the chain L .

This limit is finite and depends only on x and the trap size l . We expect that in the TSS limit

$$s_\alpha(x) \approx f_\alpha(X), \quad X \equiv x/\xi_1, \quad (20)$$

i.e., they are scaling functions of X . Note that the distance of the site $L/2 - x$ from the center of the trap is actually $y = x + 1/2$, but the effects of this difference disappears in the TSS limit $\xi_1 \rightarrow \infty$ at fixed $X \equiv y/\xi_1$, as $O(\xi_1^{-1})$. The large- p limits of f_α coincide, indeed, since $\xi_1 \rightarrow L$, (11) implies

$$\lim_{p \rightarrow \infty} f_\alpha(X) = \ln \cos(\pi X) \quad (21)$$

with $|X| < 1/2$. Corrections to scaling are again expected to be $O(l^{-\theta/\alpha})$.

In figure 3 we show data for $p = 2$, $\gamma = 1$, $l = 4000$ and a few values of the size of the chain L . They show the effects of the finite size L of the chain, and that accurate results for larger and larger X require larger and larger L . However, such effects can be carefully controlled, so that the results that we will present can be effectively considered as infinite-chain results. ⁺ We used chains of size up to $L = 4000$ for $\gamma = 1$ and up to $L = 6000$ for $\gamma = 4$, which ensure negligible finite- L effects at the trap size considered.

The numerical results for the von Neumann entropy, reported in figure 4 for $p = 2$ and $p = 4$, show that $s_1(x)$ approaches a scaling function of $X \equiv x/\xi_1$ in the TSS limit (more precisely, a function of X^2 , since it is an even function of X), which is universal, i.e., independent of γ . In figure 4 we also show extrapolations to $l \rightarrow \infty$ assuming $O(l^{-\theta})$ corrections. They are consistent with a universal TSS limit independent of γ . With

⁺ The comparison of data in Fig. 3 shows that we can obtain very accurate results around the middle of the trap even without requiring $l \ll L$, as one might naively expect. This is essentially related to the fact that the relevant length scale of the critical correlations behaves as $\xi \sim l^\theta$ and $\theta < 1$, so that we can have $\xi \ll L$ even when $l \approx L$. Note that, with increasing the power p of the confining potential, θ increases and approaches one, thus larger chain sizes are required at fixed trap size (we recall that for $p \rightarrow \infty$ we have the formal correspondence $L = 2l$).

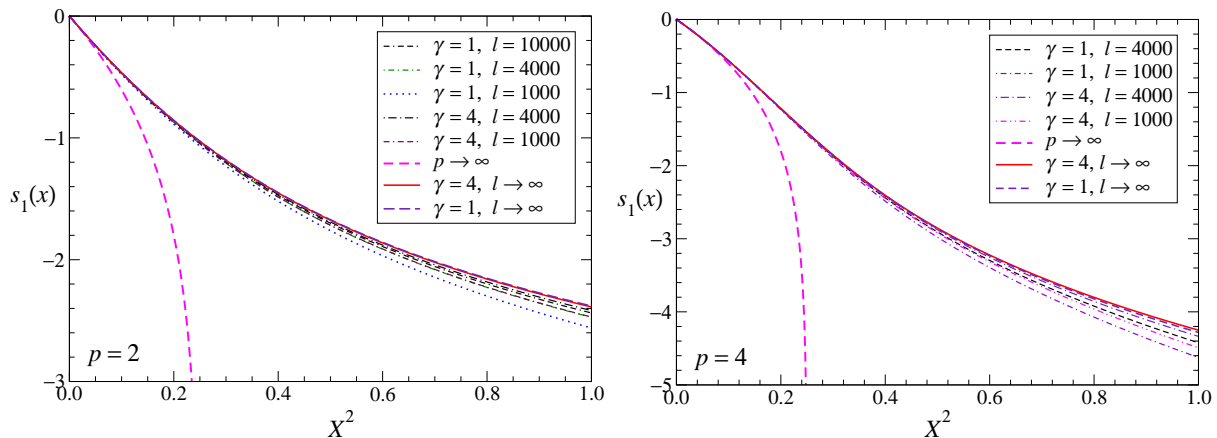


Figure 4. The function $s_1(x)$, cf. (19), vs. X^2 , for $p = 2, 4$, $\gamma = 1, 4$, and a few values of l . Curves for $l \rightarrow \infty$ are obtained by using the data for the three largest values of l , extrapolating at fixed X using the second-order polynomial $\sum_{n=0}^2 c_n l^{-n\theta}$. The extrapolated curves of data at $\gamma = 1, 4$ can be hardly distinguished, supporting the universality of the TSS. For comparison we also show the $p \rightarrow \infty$ limit (21).

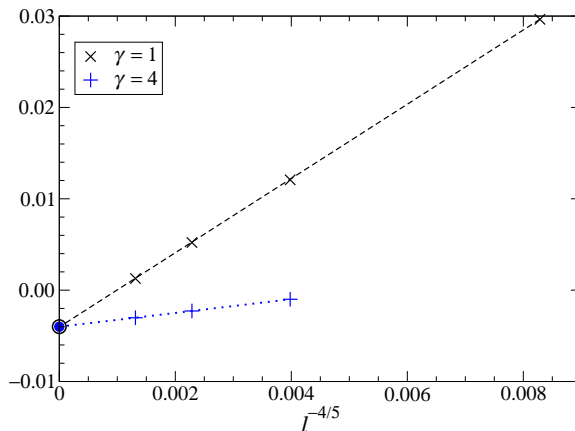


Figure 5. Results for $c_2 - c_2|_{p \rightarrow \infty} = c_2 + \pi^2/2$, cf. (22), for $p = 4$, using data for $\gamma = 1, 4$, versus $l^{-\theta}$. The crosses indicate the estimates of c_2 from polynomial fits of $s_1(x)$ at small x , which are expected to converge to its $l \rightarrow \infty$ with $O(l^{-\theta})$ corrections. The lines show linear fits of these data to $c_2 + a_\gamma l^{-\theta}$. The blobs along the y -axis show the estimates of c_2 from the fits of the $l \rightarrow \infty$ extrapolated curves of $s_1(x)$ for $\gamma = 1, 4$. The overall agreement with a universal value of c_2 is very accurate, leading to the estimate $c_2 - c_2|_{p \rightarrow \infty} \approx -0.0040$.

increasing p , the curves approach the $p \rightarrow \infty$ limit (21). The approach is particularly fast at small X , where we find

$$f_1(X) = c_2 X^2 + O(X^4) \quad (22)$$

with $c_2 \approx -4.988$ for $p = 2$ and $c_2 \approx -4.939$ for $p = 4$ (see figure 5), to be compared with $c_2 = -\pi^2/2 \approx -4.93480$ for $p \rightarrow \infty$, obtained by expanding equation (21).

Analogous results are obtained from the Rényi entropies, see figures 6 and 7, respectively for $\alpha = 2$ and $\alpha = 3$. In these cases the approach to the large- l limit is slower, because corrections are $O(l^{-\theta/\alpha})$. As a consequence the $l \rightarrow \infty$ extrapolations

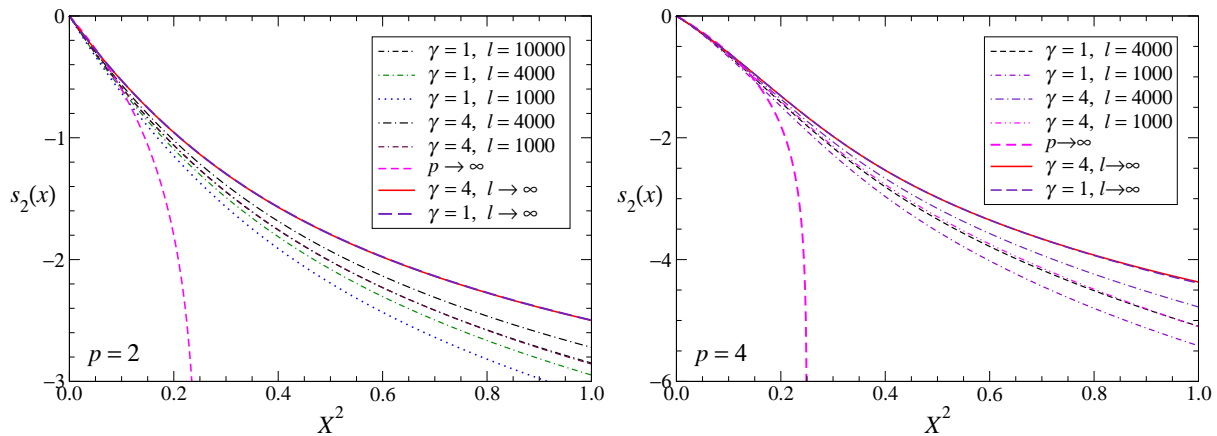


Figure 6. The function $s_2(x)$, cf. (19), vs. X^2 , for $p = 2, 4$, $\gamma = 1, 4$, and a few values of l . Curves for $l \rightarrow \infty$ are obtained by using the data for the three largest values of l , extrapolating at fixed X using the second-order polynomial $\sum_{n=0}^2 c_n l^{-n\theta/2}$. The extrapolated curves of data at $\gamma = 1, 4$ can be hardly distinguished, supporting the universality of the TSS. For comparison we also show the $p \rightarrow \infty$ limit (21).

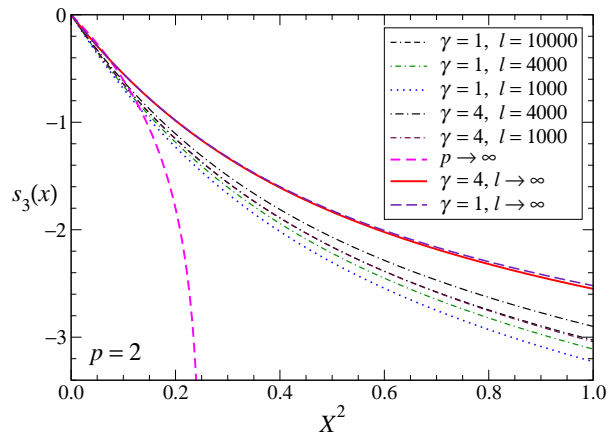


Figure 7. The function $s_3(x)$, cf. (19), vs. X^2 , for $p = 2$, $\gamma = 1, 4$, and a few values of l . Curves for $l \rightarrow \infty$ are obtained by using the data for the largest values of l , extrapolating at fixed X using the polynomials $\sum_{n=0}^{\bar{n}} c_n l^{-n\theta/3}$ with $\bar{n} = 2$ for $\gamma = 4$ and $\bar{n} = 3$ for $\gamma = 1$. For comparison we also show the $p \rightarrow \infty$ limit (21).

tend to be more imprecise with increasing α , see indeed the case $\alpha = 3$ in figure 7. Larger values of α would require larger trap sizes to get reliable $l \rightarrow \infty$ extrapolations, due to the slowly decaying $O(l^{-\theta/\alpha})$ scaling corrections. Comparing the results for $\alpha = 1, 2, 3$, we see that the functions $f_\alpha(X)$ turn out to depend little on α .

3. The 1D hard-core Bose-Hubbard model with a trapping potential

We now consider the 1D Bose-Hubbard (BH) model (1), which is of experimental relevance because it describes quasi-one-dimensional cold atoms in optical lattices, see, e.g., Refs. [6, 9, 10, 11, 17]. We consider its hard-core limit $U \rightarrow \infty$, which implies that the particle number is restricted to the values $n_i = 0, 1$, and allows us to study the

effects of the confining potential by very accurate numerical results.

The hard-core limit of the 1D BH model can be mapped into the XX chain model with a space-dependent transverse external field,

$$H_{\text{XX}} = -\frac{J}{4} \sum_i (\sigma_i^x \sigma_{i+1}^x + \sigma_i^y \sigma_{i+1}^y) - \frac{1}{2} \sum_i [\mu + V(x_i)] \sigma_i^z, \quad (23)$$

(which is the Hamiltonian (5) with $\gamma = 0$, apart from a factor 2). The Pauli spin matrices are related to the boson operators of the BH Hamiltonian H_{BH} , cf. (1), by $\sigma_i^x = b_i^\dagger + b_i$, $\sigma_i^y = i(b_i^\dagger - b_i)$, $\sigma_i^z = 1 - 2b_i^\dagger b_i$. One can then map the XX chain into a model of free spinless fermions by a Jordan-Wigner transformation, given by (6) for $\gamma = 0$ (apart from a factor 2).

In the absence of the trap, the 1D hard-core BH model has three phases: two Mott insulator phases, for $\mu > 1$ with $\langle n_i \rangle = 0$ (empty state) and for $\mu < -1$ with $\langle n_i \rangle = 1$, separated by a gapless superfluid phase for $|\mu| < 1$ characterized by the filling factor

$$f \equiv \langle n_i \rangle = (1/\pi) \arccos \mu. \quad (24)$$

A general analysis of the trap-size dependence and TSS at the Mott transitions and within the superfluid phase of the hard-core BH model (1) has been presented in Ref. [22]. Here we focus on the behaviour of the quantum entanglement within the superfluid phase, i.e., for $|\mu| < 1$, whose continuum limit is described by a free massless bosonic field theory with dynamic exponent $z = 1$, thus a conformal field theory with $c = 1$. Specifically, we consider the model at $\mu = 0$, corresponding to half filling in the absence of the trap.

3.1. Modulated multi-TSS in the superfluid phase

The trap-size dependence shows subtle effects in the parameter region where the homogeneous model without trap has a nonzero filling f , i.e., for $\mu < 1$, including the superfluid phase. This is essentially related to the presence of level crossings of the lowest states at finite trap size. They arise because the particle number is conserved, i.e., the particle number operator $\hat{N} = \sum_i n_i$ commutes with the BH Hamiltonian (1) even in the presence of the trapping potential; thus the eigenvectors do not depend on μ , even though the eigenvalues do. In the presence of the trapping potential (2), the particle number $N \equiv \langle \hat{N} \rangle$ is finite and increases as $N \sim l$ with increasing the trap size l , see (29). Therefore, as $l \rightarrow \infty$, there is an infinite number of ground-state level crossings where N jumps by 1 and the gap vanishes. In spite of the presence of these level crossings, the length scale of the critical modes diverges only in the large trap-size limit. Note that the hard-core limit, $U \rightarrow \infty$ in (1), or the spatial dimension do not play any special role, so we expect that level crossings at finite trap size are a general feature of the BH model (1) in the presence of a confining potential, when the homogeneous limit of infinite trap size has a finite particle density. The main effect of the infinite level crossings in the limit $l \rightarrow \infty$ is that the asymptotic power law behaviours get modulated by periodic functions of the trap size l , giving rise to a modulated TSS.

Moreover, in the superfluid region, the scaling of the spatial dependence of the correlation functions is characterized by two independent length scales having different power-law divergences in the large trap-size limit. One of them scales as

$$\xi_s \sim l \quad (25)$$

and describes the behaviour of observables related to smooth modes, such as the gap and the half-lattice entanglement entropy; the other one scales as

$$\xi_F \sim l^\zeta, \quad \zeta = p/(p+1), \quad (26)$$

and it is found in observables involving the modes at the Fermi scale $k_F = \pi f$, such as the density-density correlation. This gives rise to a multi-TSS behaviour, which is more complicated than that described by the scaling Ansatz (7) which applies to the XY chain model around its quantum critical point.

As we shall see, the behaviour of the quantum entanglement of parts of the system in its ground state reflects the above general features.

In the following we briefly mention a number of results obtained in Ref. [22] which will be useful for the discussion of the quantum entanglement.

The particle density of the 1D hard-core BH model approaches its local density approximation (LDA) in the large- l limit, i.e., the value of the particle density of the homogeneous system at the effective chemical potential

$$\mu_{\text{eff}}(x) \equiv \mu + (x/l)^p. \quad (27)$$

The LDA of the particle density reads

$$\langle n_x \rangle_{\text{lda}} \equiv \rho_{\text{lda}}(x/l) = \begin{cases} 0 & \text{for } \mu_{\text{eff}}(x) > 1, \\ (1/\pi) \arccos \mu_{\text{eff}}(x) & \text{for } -1 \leq \mu_{\text{eff}}(x) \leq 1, \\ 1 & \text{for } \mu_{\text{eff}}(x) < -1. \end{cases} \quad (28)$$

Corrections are generally suppressed by powers of the trap size, and present a nontrivial scaling behaviour [22] in term of the scaling variable $Y \equiv x/l^\zeta$.

Asymptotically, the total particle number is obtained by integrating the local density approximation of the particle density ρ_{lda} :

$$N \equiv \langle \hat{N} \rangle = c_\mu l + O(1), \quad c_\mu = 2 \int_0^\infty \rho_{\text{lda}}(y) dy. \quad (29)$$

At $\mu = 0$ we have $c_{\mu=0} \approx 0.76276$ for $p = 2$, $c_{\mu=0} \approx 0.859407$ for $p = 4$, and $c_{\mu=0} \rightarrow 1$ for $p \rightarrow \infty$.

In the superfluid region the interval between subsequent level crossings $l_0^{(k)}$ (where k enumerates them with increasing trap size) tends to a constant value in the large trap-size limit, given by [22]

$$\lim_{k \rightarrow \infty} \left(l_0^{(k+1)} - l_0^{(k)} \right) = 1/c_\mu, \quad (30)$$

with $O(l^{-2})$ corrections (this formula has been checked with great accuracy by numerical computations). In the limit $p \rightarrow \infty$ the interval of level crossings converges toward the

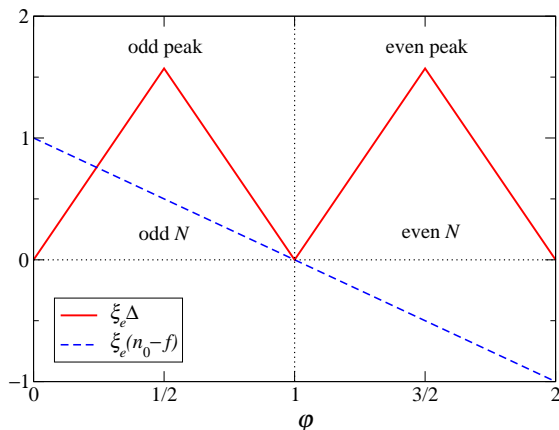


Figure 8. The asymptotic behaviour of the gap and the particle density at the center of the trap at $\mu = 0$, thus $f = 1/2$. In formulae [22], $\Delta = \pi t(\varphi)/\xi_e$ and $\langle n_0 \rangle - f = (1 - \varphi)/\xi_e$, where ξ_e is the entanglement length scale defined in (38). These results apply for any p , including $p \rightarrow \infty$.

corresponding value in the finite-size behaviour of the homogeneous system with open boundary conditions, which is $1/(2f)$.

The amplitudes of the asymptotic power law behaviours turn out to be modulated by periodic functions of the trap size, whose period is related to the level crossing interval (30). In order to describe such phenomenon, since some quantities distinguish between odd and even level crossings, we introduce the phase-like variable

$$\varphi = 2 \frac{l - l_0^{(2k)}}{l_0^{(2k+2)} - l_0^{(2k)}} \quad \text{for } l_0^{(2k)} \leq l < l_0^{(2k+2)}, \quad (31)$$

thus $0 \leq \varphi < 2$. φ provides the normalized distance from the largest even level crossing smaller than the given l .^{*} Values in the range $0 \leq \varphi \leq 1$ corresponds to ground states with odd particle numbers, while the range $1 \leq \varphi \leq 2$ corresponds to even particle numbers. Note that (30) implies that φ is a periodic function of l in the asymptotic regime.

In the superfluid phase, i.e. $|\mu| < 1$, the asymptotic behaviours of the gap and the particle density at the center of the trap are given by

$$\begin{aligned} \Delta &\sim t(\varphi)l^{-1}, & t(\varphi) &= 1/2 - ||1 - \varphi| - 1/2|, \\ \langle n_0 \rangle - f &\sim (1 - \varphi)l^{-1}, \end{aligned} \quad (32)$$

respectively. The amplitudes of the asymptotic power-law behaviours get modulated by periodic functions of the trap size, through the dependence of φ of their amplitudes. The values $\varphi = 1/2$ and $\varphi = 3/2$ correspond to the odd and even peaks of the gap, where the particle number $N = \langle \hat{N} \rangle$ is odd and even respectively. In figure 8 we show their behaviours at $\mu = 0$.

An analogous modulation of the asymptotic behaviours is found in the limit $p \rightarrow \infty$, i.e. for a homogeneous chain of size L with open boundary conditions [22]. In this case,

^{*} In Ref. [22] the variable φ was denoted by $\bar{\phi}$.

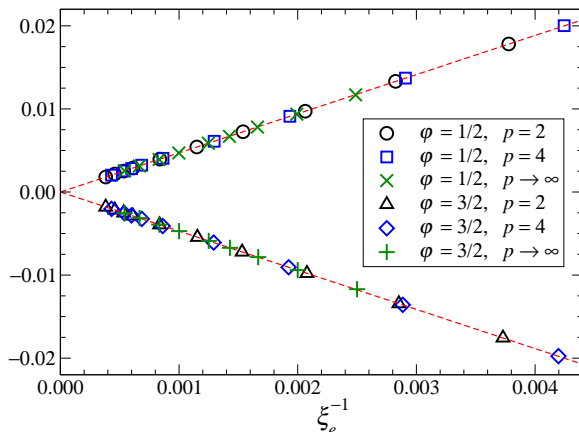


Figure 9. The quantity $\xi_e(6S_{1,1/2} - \ln \xi_e - e_1)$, for $\varphi = 1/2, 3/2$ and $p = 2, 4, \infty$. The dashed lines show the linear behaviour $\pm 3\pi/(2\xi_e)$ for $\varphi = 1 \mp 1/2$, in agreement with (37).

the variable φ reads

$$\varphi \equiv 2\{[(L+1)f + 1]/2\}, \quad (33)$$

where $\{x\} \equiv x - [x]$ is the fractional part of x (i.e., the sawtooth function). The asymptotic behaviour of the gap is given by

$$\Delta = \pi(1 - \mu^2)^{1/2} t(\varphi) L^{-1}. \quad (34)$$

At $\mu = 0$, i.e., $f = 1/2$, the variable φ takes only discrete values: $\varphi = 0, 1/2, 1, 3/2$ (the values $1/2$ and $3/2$ corresponds to even chain size, with odd and even particle number respectively).

3.2. Asymptotic trap-size dependence of the bipartite entanglement entropies

Let us consider a chain with even L sites and open boundary conditions, and a trap of size l centered between the middle sites of the chain. We again divide it into two subsystems and study the behaviours of the von Neumann and Rényi entropies of one of the subsystems. We present results up to trap sizes $l = O(10^3)$, corresponding to total particle numbers of $O(10^3)$, see equation (29). We used chains of size up to $L = 3000$ to achieve negligible finite- L effects (a more detailed discussion of this point for the XX chain can be found in the App. A of Ref. [22]).

In the absence of the trap, the behaviour of the entanglement entropies is given by (11) with $c = 1$, with

$$e_\alpha = \ln \sqrt{1 - \mu^2} + \ln(4/\pi) + y_\alpha, \quad (35)$$

obtained using the results of Refs. [4, 28, 29]. Corrections are again expected to be $O(L^{-1/\alpha})$ [31, 30]. The large- L behaviour of numerical results is indeed compatible with

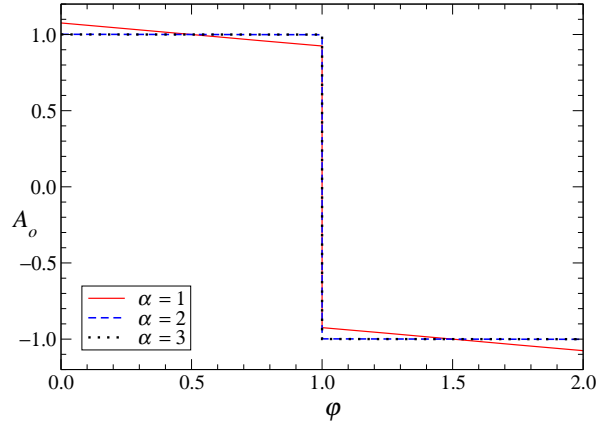


Figure 10. The function $A_o(\varphi)$ as obtained from data at $l \approx 998$, normalized so that $A_o(1/2) = 1$ and $A_o(3/2) = -1$.

the following asymptotic behaviour

$$S_\alpha(L/2 - x; L) = C_\alpha \left[\ln(L+1) + \ln \cos(\pi X) + e_\alpha - (-1)^{L/2-x} \frac{b_\alpha}{(L \cos \pi X)^{1/\alpha}} + O(L^{-2/\alpha}) \right] \quad (36)$$

with $X \equiv x/(L+1)$, and $b_1 = 3\pi/2 \approx 4.71239$, $b_2 \approx 4.79256$ and $b_3 \approx 4.19726$. Note that the factor $L+1$ in the logarithm and in the definition of X is essential to get a formula which is correct up to $O(L^{-2})$ at fixed X in the case of the von Neumann entropy ($\alpha = 1$).

The half-lattice von Neumann entropy in the presence of the trap was already considered and numerically investigated in Ref. [22], finding an entanglement length scale which increases linearly with the trap size in the whole superfluid region. Specifically, at $\mu = 0$ and for any power p of the potential, including $p \rightarrow \infty$, the half-lattice von Neumann entropy behaves as [22]

$$S_{1,1/2} = \frac{1}{6} \left[\ln \xi_e + e_1 + A_o(\varphi) \frac{3\pi}{2\xi_e} + O(\xi_e^{-2}) \right], \quad (37)$$

where

$$\xi_e = a_e l, \quad a_e = \sqrt{\pi} \Gamma\left(\frac{1}{2p}\right) \left[p \Gamma\left(\frac{1+p}{2p}\right) \right]^{-1}. \quad (38)$$

ξ_e provides an entanglement length scale, and $A_o(\varphi)$ is a periodic function of l which can be parametrized by

$$A_o(\varphi) = \begin{cases} 1 + q(\varphi - 1/2) & \text{for } 0 < \varphi < 1, \\ -1 - q(3/2 - \varphi) & \text{for } 1 < \varphi < 2 \end{cases} \quad (39)$$

Note that $A_o(1 \mp 1/2) = \pm 1$. In figure 9 we show results for $p = 2, 4, \infty$ and $\varphi = 1/2, 3/2$. They clearly support equation (37). The function $A_o(\varphi)$ is shown in figure 10 for $p = 2$ for trap sizes around $l \approx 998$. We estimate $q \approx -0.152$ for $p = 2$ and $q \approx -0.044$ for $p = 4$. The parametrization (39) of $A_o(\varphi)$ is convenient when

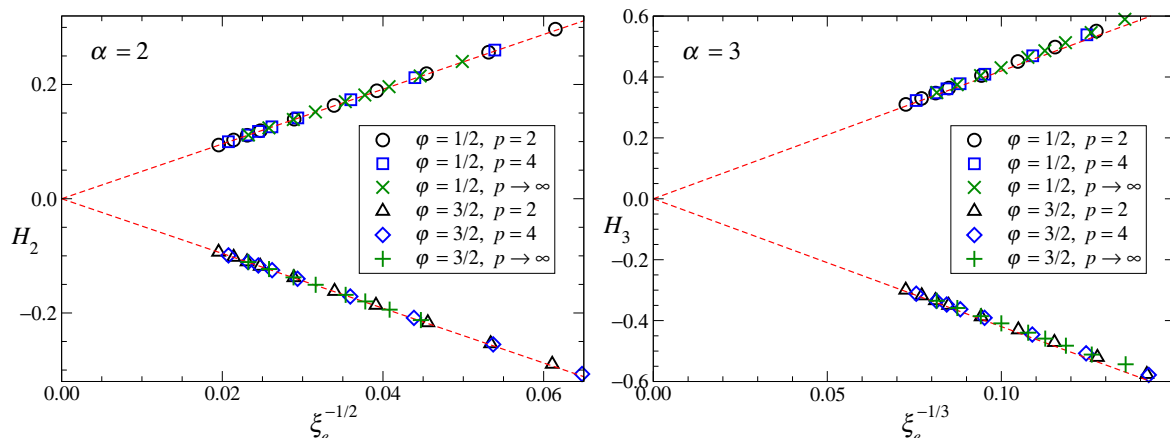


Figure 11. The quantity H_α , defined in (40), for $\alpha = 2, 3$, $\varphi = 1/2, 3/2$ and $p = 2, 4, \infty$. The dashed lines show the linear behaviour $\pm b_\alpha \xi_e^{-1/\alpha}$ for $\varphi = 1 \mp 1/2$, with $b_2 = 4.79256$ and $b_3 = 4.19726$, cf. (41).

comparing with the $p \rightarrow \infty$ limit, because $\varphi = 1/2, 3/2$ are the only possible values for the homogeneous system in a chain with even L , corresponding to odd and even $L/2$ (thus odd and even particle number N) respectively. The behaviour of the homogeneous system with open boundary condition, cf. (11), is obtained by replacing $\xi_e \rightarrow L + 1$ at the values $\varphi = 1/2, 3/2$.

We now show that the half-lattice Rényi entropies show analogous behaviours. In figure 11 we show numerical results of the quantity

$$H_\alpha \equiv \xi_e^{1/\alpha} (C_\alpha^{-1} S_{\alpha,1/2} - \ln \xi_e - e_\alpha) \quad (40)$$

for $p = 2, 4, \infty$ and $\varphi = 1/2, 3/2$. The data appears to follow curves which are apparently independent of p , but clearly depending on φ . Therefore, analogously to the case of the von Neumann entropy, the asymptotic behaviour of the Rényi entropies show the same form for any value of the potential power p , including $p \rightarrow \infty$, when they are expressed in terms of the entanglement length scale ξ_e , i.e.,

$$S_{\alpha,1/2} = C_\alpha [\ln \xi_e + e_\alpha + b_\alpha A_{\alpha,o}(\varphi) \xi_e^{-1/\alpha} + O(\xi_e^{-2/\alpha})] \quad (41)$$

where b_α are the same constants entering the behaviour of the half-lattice Rényi entanglement entropies of the homogeneous system, cf. (36), and $A_{\alpha,o}$ is given by (39), with very small values of q , i.e. $q \approx -0.003$ for $\alpha = 2, p = 2$ and $q \approx -0.001$ for $\alpha = 3, p = 2$. Thus $A_{\alpha,o} \approx (-1)^N$ for $\alpha > 1$. Equations (37) and (41) imply that the length scales defined in (14) behave as

$$\xi_\alpha = \xi_e [1 + O(\xi_e^{-1/\alpha})] \quad (42)$$

for any α .

We now analyze the spatial dependence of the bipartite entanglement entropies. We again consider the functions defined in (19). In figures 12, 13, and 14 we show results for $p = 2, 4, \alpha = 1, 2, 3, \varphi = 1/2, 3/2$, and several values of the trap size. In all cases the behaviours of the functions $s_\alpha(x)$, defined as in (19), are characterized by a

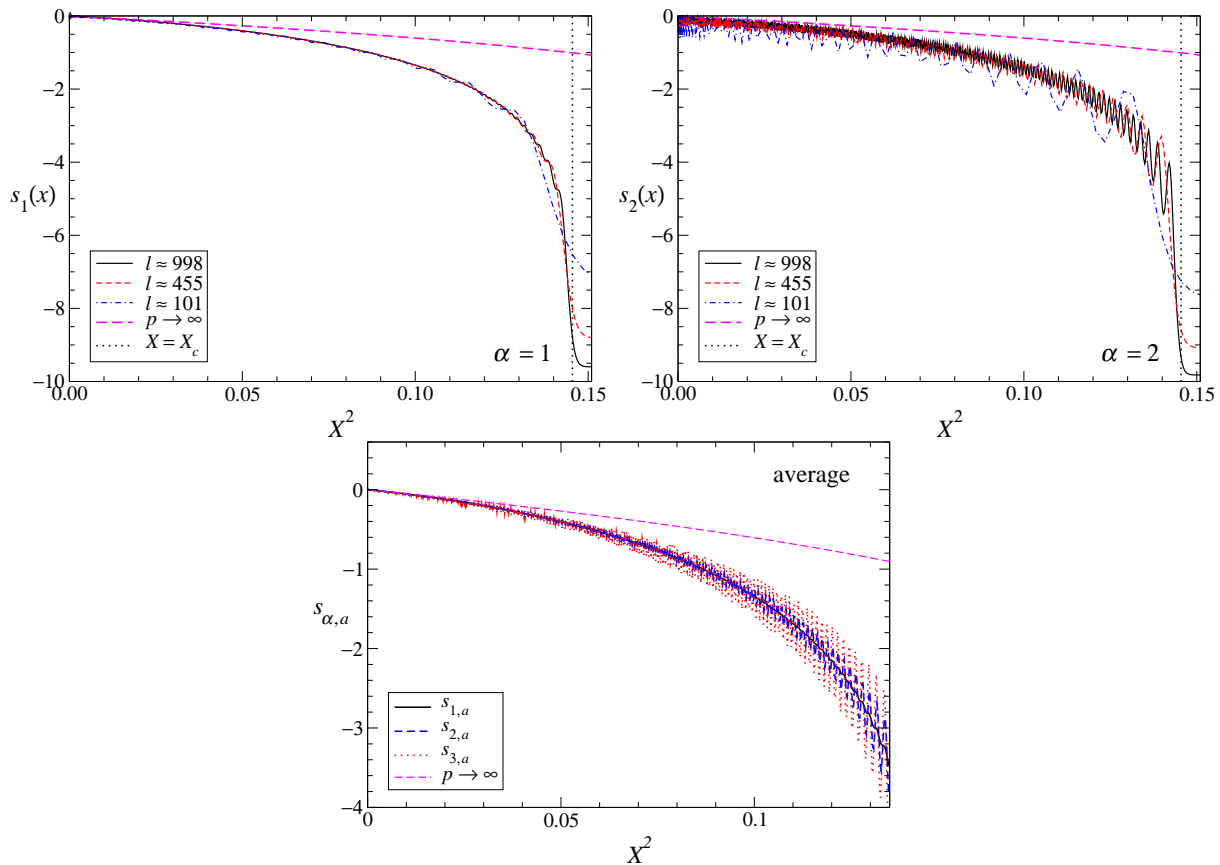


Figure 12. s_α vs. X^2 , for $\alpha = 1, 2, 3$, $p = 2$, $\varphi = 1/2$, and a few values of l . The vertical dotted lines show the value $X = X_c = 1/a_e$, cf. (38).

smooth function $f_\alpha(X)$ with $X \equiv x/\xi_e$, and oscillations around it, which appear larger and larger with increasing α , but get suppressed with increasing ξ_e . These numerical results suggest

$$s_\alpha(x) = f_\alpha(X) + O(\xi_e^{-1/\alpha}), \quad X \equiv x/\xi_e, \quad (43)$$

where the power-law of the corrections can be guessed from the fact that $O(L^{-1/\alpha})$ corrections are expected in homogeneous system with open boundary conditions [31, 30]. Moreover, the numerical results strongly suggest that a unique function describes the leading behaviour for any α , i.e., $f_\alpha(X) \equiv f(X)$ is independent of α , for any p . This becomes more evident when considering the average $s_{\alpha,a}$ of the functions $s_\alpha(x)$ at subsequent odd and even peaks of the gap (indeed, as we shall see below, the curves at $\varphi = 1/2$ and $\varphi = 3/2$ have opposite oscillating corrections at least for sufficiently small values of X). With increasing p the function $f(X)$ appears to tend to the $p \rightarrow \infty$ limit given by (21). Actually, the small- X behaviour at $p = 2$ is already very close to the $p \rightarrow \infty$ limit (the large- l extrapolation of the coefficient c_2 of the $O(X^2)$ term is compatible with its $p \rightarrow \infty$ limit $c_2 = -\pi^2/2$ already at $p = 2, 4$). On the other hand, oscillations are strongly dependent on α .

An interesting numerical relation concerning the leading behaviour $f(X)$ is illustrated in figure 15: for $p = 2, 4, 6$, we find that the difference between $f(X)$

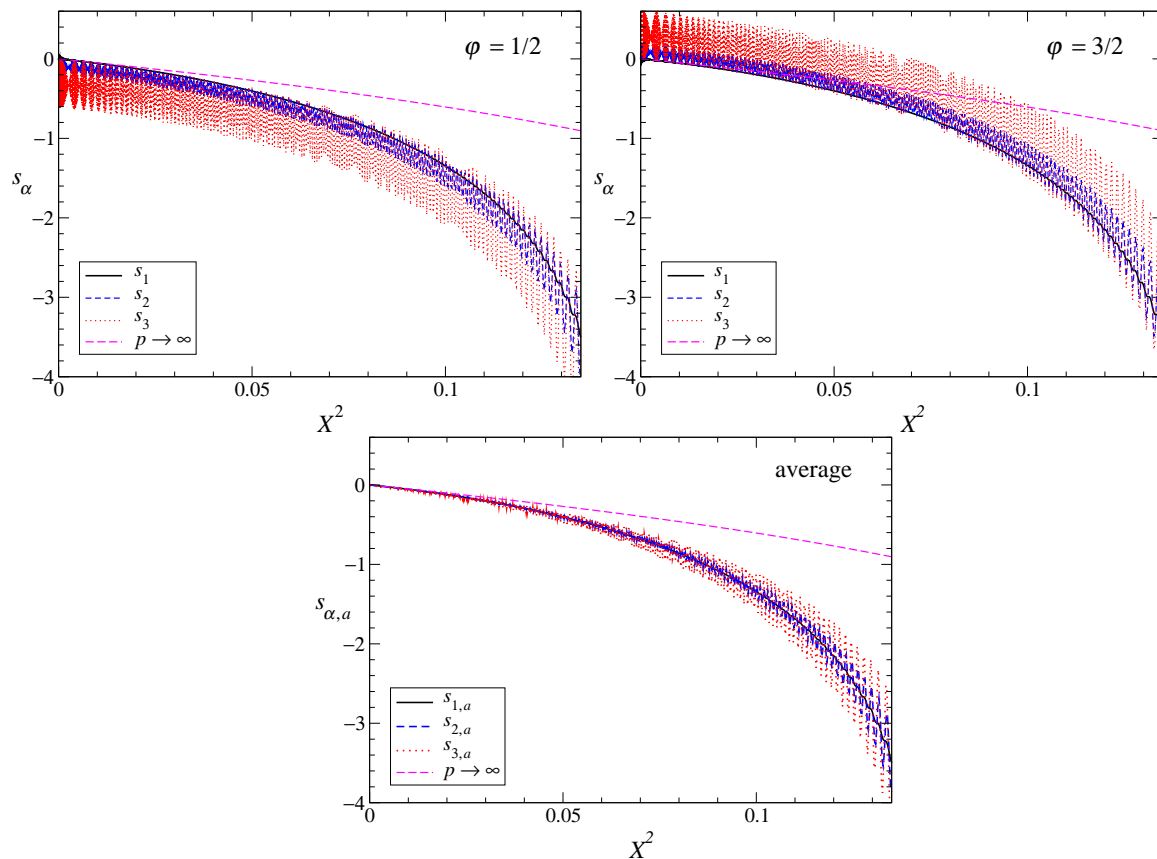


Figure 13. s_α vs. X^2 for $\alpha = 1, 2, 3$, $p = 2$, and $l \approx 10^3$, at $\varphi = 1/2$, $\varphi = 3/2$, corresponding to $N = 761, 762$, and their average $s_{\alpha,a} \equiv (s_\alpha|_{\varphi=1/2} + s_\alpha|_{\varphi=1/3})/2$, which has much smaller oscillations.

and its $p \rightarrow \infty$ limit given by CFT, i.e. $\lim_{p \rightarrow \infty} f(X) = \ln \cos \pi X$, is a function of $\mu_{\text{eff}} \equiv (|x|/l)^p = (a_e X)^p$ only, i.e.,

$$f(X) \approx \ln \cos \pi X + A(\mu_{\text{eff}}) \quad (44)$$

where the (p -independent) function A behaves as $A(\mu_{\text{eff}}) = O(\mu_{\text{eff}}^2)$ at small X (more precisely the numerical results indicate $A(\mu_{\text{eff}}) = a\mu_{\text{eff}}^2 + O(\mu_{\text{eff}}^4)$ with $a \approx -1.0$).

Note that the von Neumann and Rényi entropies rapidly decrease around $X = X_c$ corresponding to $x_c \equiv l$, thus $X_c = 1/a_e$, cf. (38); x_c is the value of x where $\mu_{\text{eff}}(x) = (x/l)^p = 1$, i.e., the value of the chemical potential corresponding to the superfluid to empty state transition, where the particle density of the ground state vanishes, see equation (28). We thus expect that, for generic values of μ and p , the region around $x = x_c$ develops critical modes related to a low-density Mott transition from the superfluid phase to the empty state. The effective chemical potential can be expanded around x_c as

$$\mu_{\text{eff}} = (x/l)^p = 1 + p \frac{x - x_c}{l} + O[(x - x_c)^2]. \quad (45)$$

Thus, the behaviour around x_c is essentially analogous to that arising at the low-density Mott transition $\mu = 1$ in the presence of a linear potential $V_l \sim r/l$. Around x_c , critical

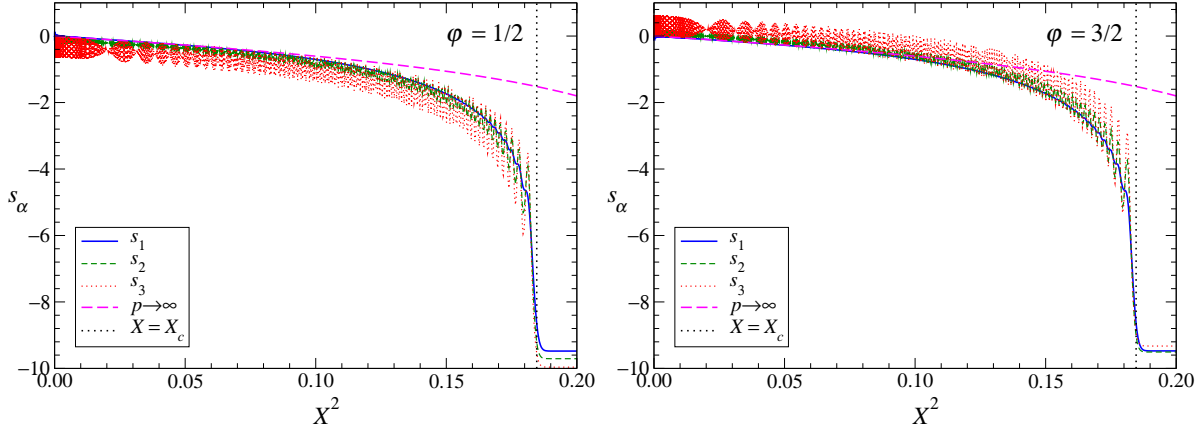


Figure 14. s_α vs. X^2 for $\alpha = 1, 2, 3$, $p = 4$, $l \approx 10^3$, and $\varphi = 1/2, 3/2$, corresponding to $N = 857, 856$. The vertical dotted lines show the value $X = X_c = 1/a_e$, cf. (38).

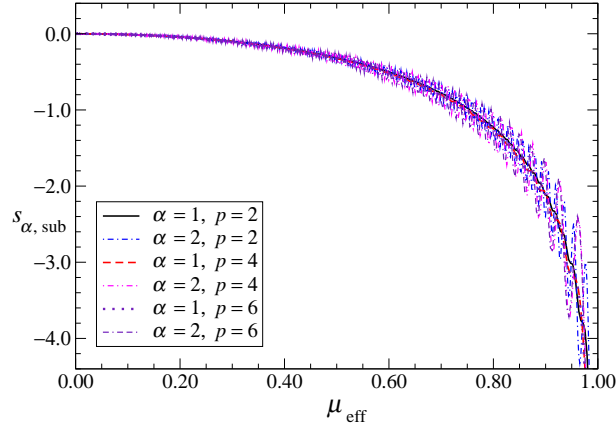


Figure 15. $s_{\alpha,sub} \equiv \frac{1}{2}[s_\alpha(x)|_{\varphi=1/2} + s_\alpha(x)|_{\varphi=3/2}] - \ln \cos \pi X$ vs. $\mu_{\text{eff}} = (x/l)^p$ for $\alpha = 1, 2$ and $p = 2, 4$ (for $l \approx 1000$) and $p = 6$ (for $l \approx 1400$).

modes should appear with length scale $\xi \sim l^\sigma$, where σ is the exponent associated with a linear external potential. The value of σ can be inferred by RG arguments analogous to those leading to the determination of the trap exponent θ at the low-density Mott transition [20], which give $\sigma = 1/3$.[‡] We thus expect that the transition region around $x = x_c$ enlarges as

$$\Delta x \sim l^{1/3}, \quad (46)$$

independently of the power-law p of the confining potential. This behaviour is confirmed by the numerical values of $\Delta x \equiv l - x_{\text{max}}$, where x_{max} is the abscissa of the rightmost maximum of $s_\alpha(x)$, interpolated to continuous x ; figure 16 shows the perfect agreement

[‡] The exponent σ can be determined by a RG analysis of the perturbation corresponding to a linear potential $V_l(x) = ux$, i.e., $\int d^d x dt V_l(x) |\phi(x, t)|^2$, at the fixed point of the continuous theory describing the Mott transition [19]. The exponent σ is related to the RG dimension y_u of the parameter u , which can be obtained from the relations $y_u - 1 = d + z - y_{|\phi|^2} = y_\mu = 2$, thus $y_u = 3$, and therefore $\sigma \equiv 1/y_u = 1/3$ for $d = 1$ and $d = 2$.

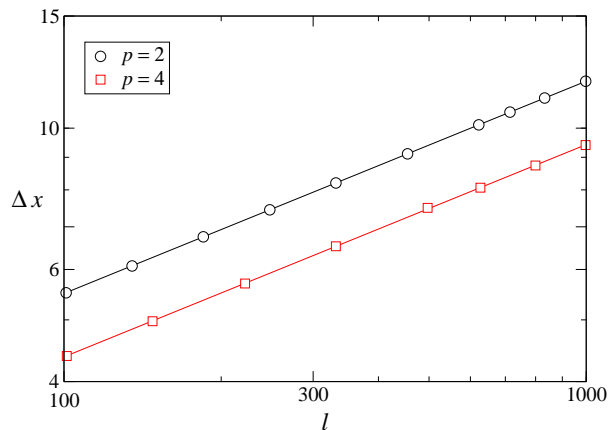


Figure 16. Δx vs. l for $\alpha = 2$, $p = 2, 4$ and $\varphi = 1/2$. The solid lines are one-parameter fits with the form $al^{1/3}$, cf. (46).

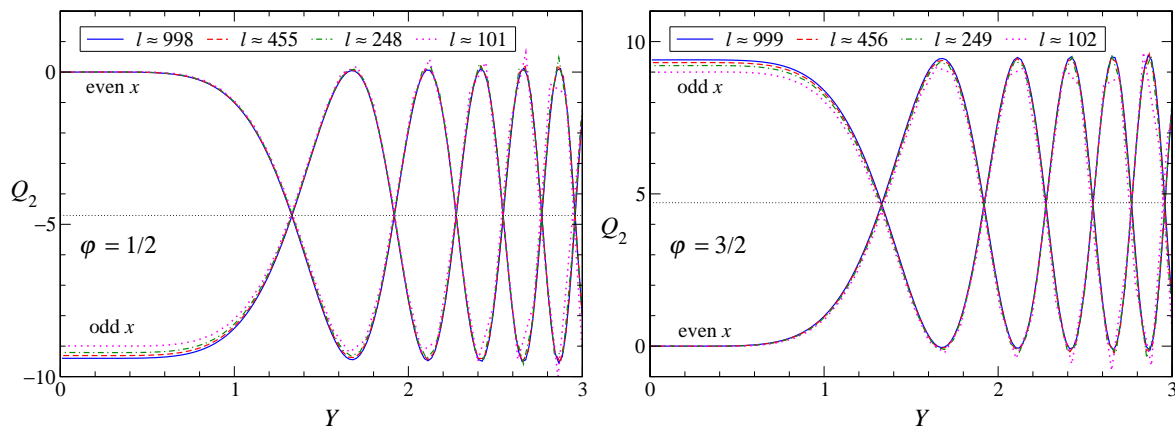


Figure 17. The function $Q_2(x)$, cf. (47), vs. $Y \equiv xl^{-2/3}$, for $p = 2$ and $\varphi = 1/2, 3/2$.

with (46).

The behaviours of the subleading and oscillating $O(\xi^{-1/\alpha})$ corrections are instead more subtle. In order to study them, we consider the function

$$Q_\alpha(x) = \xi_e^{1/\alpha} [s_\alpha(x) - s_1(x)] \quad (47)$$

for $\alpha > 1$. Assuming that the leading behaviour is given by the same function $f(X)$ for any α , Q_α should provide the $O(\xi_e^{-1/\alpha})$ term in (43). The functions $Q_\alpha(x)$ for $\alpha = 2, 3$, $p = 2, 4$, and $\varphi = 1/2, 3/2$ are shown in figures 17, 18 and 19, as obtained by numerical results at fixed trap size for $10^2 \lesssim l \lesssim 10^3$. They clearly show the expected even-odd spatial effect proportional to $(-1)^x = e^{2ik_F x}$, but also a φ -dependent scaling limit as a function of $Y = x/l^\zeta$ with $\zeta = p/(p+1)$. More precisely, the numerical results show that the asymptotic behaviour of the the functions $Q_\alpha(x)$ can be written as

$$Q_\alpha(x) \approx (-1)^x g_{\alpha,o}(Y, \varphi) + g_{\alpha,s}(Y, \varphi) \quad (48)$$

apart from further suppressed scaling corrections. Note that this strong evidence of scaling provides also an indirect and accurate check of the initial hypothesis that the

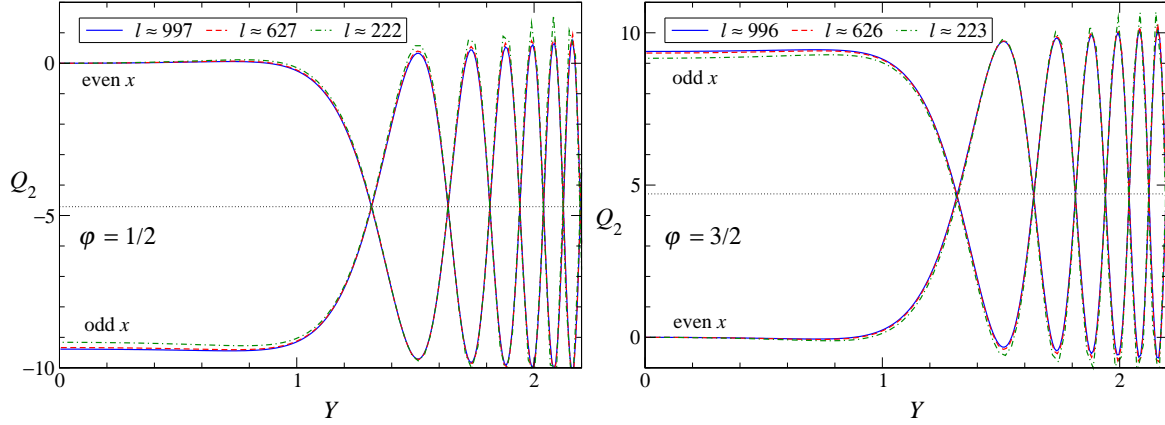


Figure 18. The function $Q_2(x)$, cf. (47), vs. $Y \equiv xl^{-4/5}$, for $p = 4$ and $\varphi = 1/2, 3/2$.

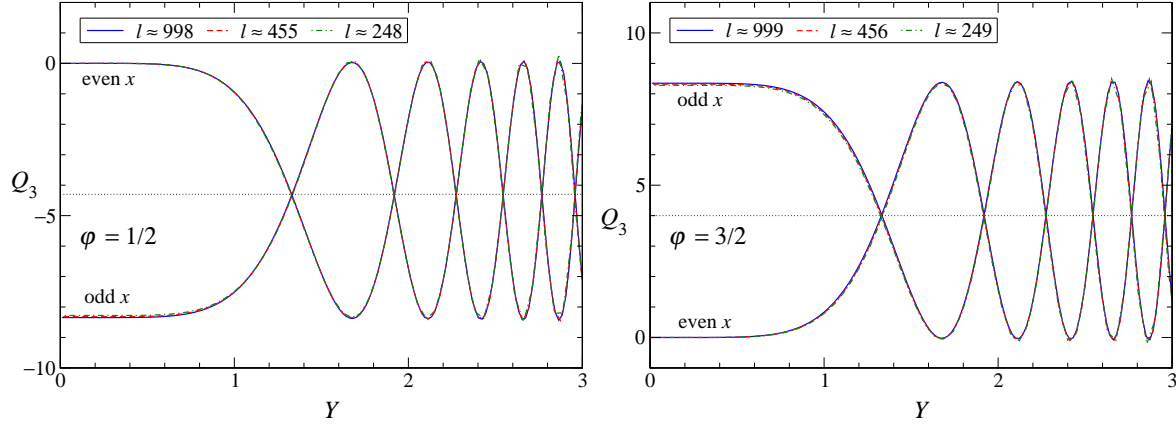


Figure 19. The function $Q_3(x)$, cf. (47), vs. $Y \equiv xl^{-2/3}$, for $p = 2$ and $\varphi = 1/2, 3/2$.

leading behaviour as a function of X does not depend on α , as in the $p \rightarrow \infty$ limit. Summarizing, we have

$$s_\alpha(x) = f(X) + \xi_e^{-1/\alpha} [(-1)^x g_{\alpha,o}(Y, \varphi) + g_{\alpha,s}(Y, \varphi)] + O(\xi_e^{-2/\alpha}) \quad (49)$$

where $X \equiv x/\xi_e$ and $Y \equiv x/l^\zeta$. We note that the behaviour of the von Neumann entropy, $\alpha \rightarrow 1$, is quite similar to that of the particle density, which turns out to be [22]

$$\langle n_x \rangle \approx \rho_{\text{lda}}(X) + \xi_e^{-1} [(-1)^x h_o(Y, \varphi) + h_s(Y, \varphi)] \quad (50)$$

Moreover, as shown by figures 20 and 21, for $p = 2$ and $p = 4$ respectively, the oscillations appear to be very close to periodic functions when plotted versus Y^{p+1} . This is particularly verified in the case of the harmonic potential, where the data at the odd and even peaks of the gap, corresponding to ground states with odd and even particle number N , accurately fit the simple function

$$Q_\alpha(x)|_{\varphi=1/2, 3/2} \approx (-1)^N b_\alpha [(-1)^x \cos(cY^3) - 1] \quad (51)$$

where b_α are the same constants entering the behaviour of the Rényi entropies of the homogeneous system, and $c \approx 2/3$. In figure 22 we show data for other values of φ .

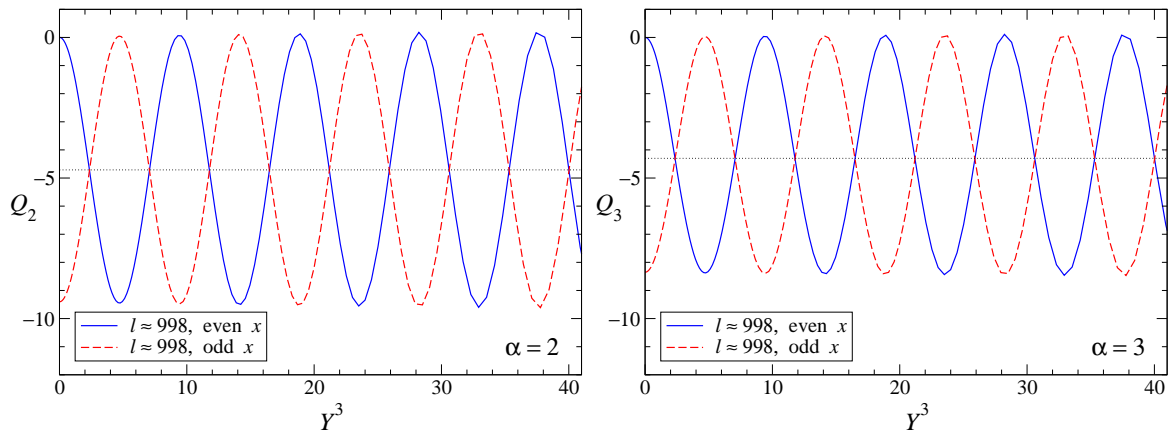


Figure 20. The functions $Q_\alpha(x)$, cf. (47), vs. $Y^3 \equiv x^3/l^2$, for $p = 2$, $\varphi = 1/2$, and $\alpha = 2, 3$.

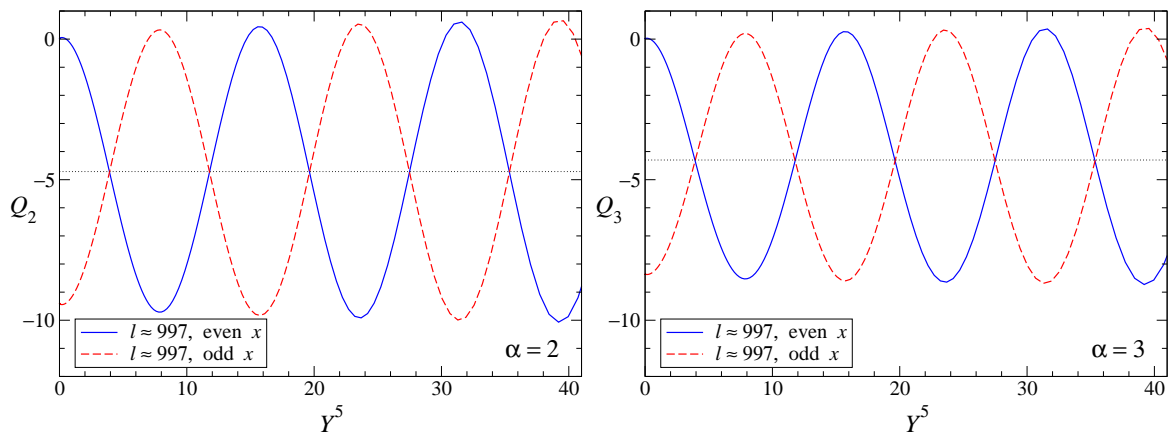


Figure 21. The functions $Q_\alpha(x)$, cf. (47), vs. $Y^5 \equiv x^5/l^4$, for $p = 4$, $\varphi = 1/2$, and $\alpha = 2, 3$.

Apart from the prefactor $(-1)^N$, there is a small residual dependence on φ , which is apparently relegated to a small dependence of c on φ .

4. Conclusions

In this paper we have investigated the scaling behaviour of the bipartite entanglement of 1D lattice systems in the presence of a power-law confining potential $V(r) = (r/l)^p$, at a quantum critical point. We have considered lattice systems whose quantum critical behaviours are described by 2D conformal field theories in the absence of the trap, thus showing logarithmically divergent entanglement entropies, see, e.g., (11).

We have considered 1D lattice models of even size L and open boundary conditions, with a trap of size l centered between the middle sites of the chain. We have divided the chain in two parts of length $l_A \equiv L/2 - x$ and $L - l_A$, and computed their von Neumann and Rényi entropies $S_\alpha(L/2 - x; L)$. In the presence of a trap of size l , the dependence on L disappears when $L \rightarrow \infty$, leaving only the dependence on x and the trap size l . We have studied the scaling behaviour of the bipartite entanglement with increasing the

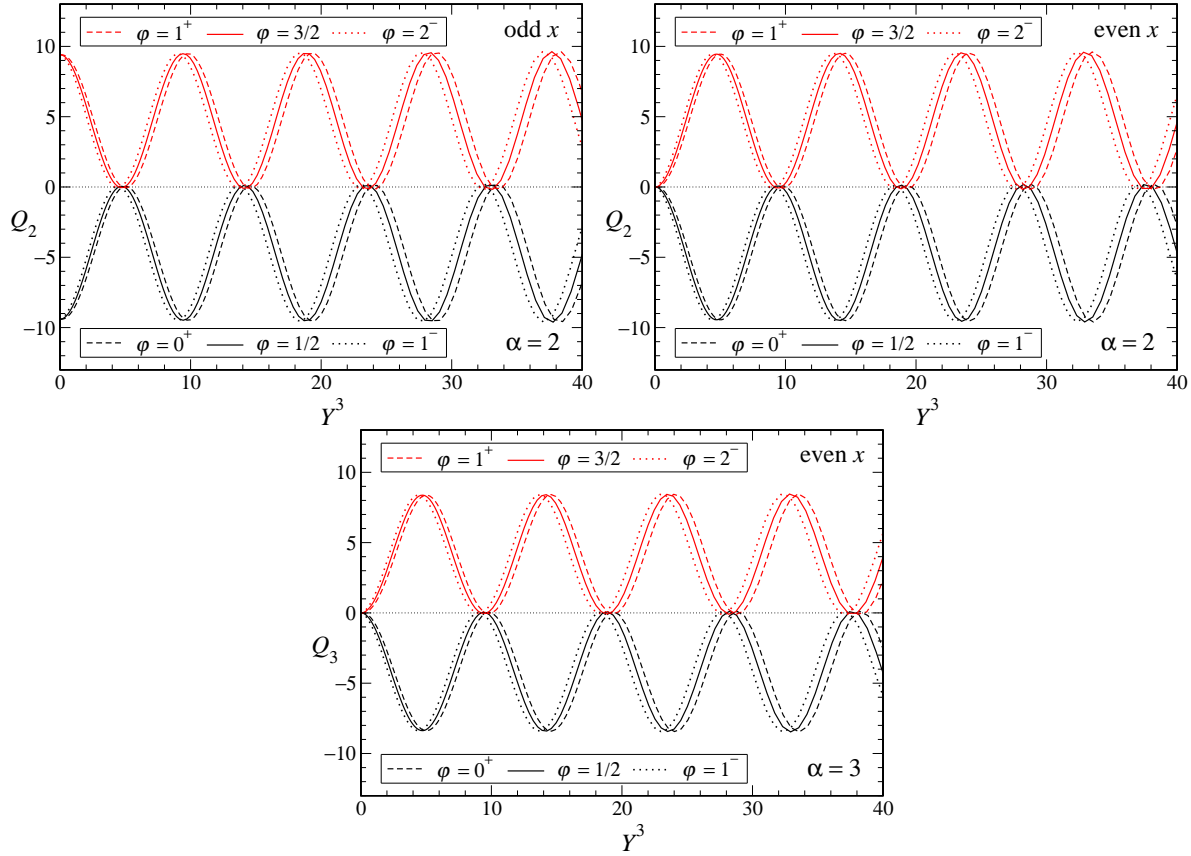


Figure 22. The functions $Q_\alpha(x)$, cf. (47), vs. $Y^3 \equiv x^3/l^2$, for $p = 2$, $\alpha = 2, 3$, several values of φ , for sites with even and odd parity, and trap sizes $l \approx 998$. Q_α as a function of φ has jumps for integer φ ; we denote $\lim_{\varphi \searrow n}$ by $\varphi = n^+$ and $\lim_{\varphi \nearrow n}$ by $\varphi = n^-$.

trap size, keeping the other model parameters fixed at the quantum critical point of the homogeneous system without trap.

As a theoretical laboratory, we have considered the quantum XY chain in an external space-dependent transverse field, acting as a trap for the spinless fermions of its quadratic Hamiltonian representation. This model presents a quantum critical transition belonging to the 2D Ising universality class, thus described by a CFT with central charge $c = 1/2$. In the presence of the trap and for large trap sizes, the quantum critical behaviour can be described in the framework of the TSS theory [20], where the quantum critical behaviour is cast in the form a TSS, cf. (7), with a nontrivial trap exponent $\theta = p/(p+1)$, which determines how the length scale of the critical modes at the critical point diverges with increasing trap size, i.e., $\xi \sim l^\theta$. Exploiting the quadratic spinless fermion representation of the XY chain, we have computed the bipartite von Neumann and Rényi entanglement entropies up to $l \approx 10^4$. Our results show that at the quantum critical point they behave as

$$\lim_{L \rightarrow \infty} S_\alpha(L/2 - x; L) = C_\alpha \left[\ln \xi_1 + \ln R_\alpha + e_\alpha + f_\alpha(X) + O(\xi_1^{-1/\alpha}) \right], \quad (52)$$

$$\xi_1 = a_1 \gamma^{\theta/p} l^\theta [1 + O(l^{-\theta})], \quad X \equiv x/\xi_1, \quad \xi_\alpha/\xi_1 = R_\alpha + O(\xi_1^{-1/\alpha}),$$

where $C_\alpha = c(1 + \alpha^{-1})/12$, $c = 1/2$ is the central charge, and e_α is the same constant entering the entanglement entropies of homogeneous systems with open boundary conditions, cf. (13). The entanglement length scales ξ_α are defined by imposing $S_\alpha(L/2; L) \equiv C_\alpha(\ln \xi_\alpha + e_\alpha)$; the length scales ξ_α , and in particular ξ_1 derived from the von Neumann entropy, behave consistently with the predictions of the TSS theory, with $\theta = p/(p+1)$ and a_1 independent of γ . The asymptotic ratios R_α and the functions $f_\alpha(X)$ depend on the power of the potential, show a small dependence on α , but are universal with respect to the parameter γ , see figures 4, 6, and 7. Moreover, in the $p \rightarrow \infty$ limit they tend to $f_\alpha(X) = \ln \cos \pi X$ with $X = x/L$, which is the behaviour in the homogeneous system with open boundary conditions.

We have studied the scaling of the entanglement of confined particle systems described by the 1D BH model (1) in the presence of a power-law confining potential, with the center of the trap in the superfluid phase. This model is of experimental relevance because it describes cold atoms in quasi-one-dimensional optical lattices. We have computed bipartite entanglement in the hard-core limit of the model, which allows very accurate numerical calculations by exploiting a map into a lattice model of free spinless fermions. In the absence of the trap, the continuum theory corresponding to the gapless superfluid phase is a 2D massless boson field theory, thus a CFT with $c = 1$. In this region the trap-size dependence presents new features with respect to the XY chain: a multiscaling behaviour with the existence of different length scales which diverge with distinct power laws in the TSS; the presence of level crossings of the lowest states at finite trap size, which gives rise to periodic modulations of the amplitudes of the asymptotic power-law behaviours, with a period given by the asymptotically constant interval between the level crossings. We have shown that the bipartite entanglement entropy presents the same features as well. We have computed the von Neumann and Rényi entropies at $\mu = 0$ corresponding to half filling $f = 1/2$ in the absence of the trap, up to trap sizes $l \approx 10^3$, corresponding to total particle numbers $N = O(10^3)$. Our results provide a robust numerical evidence of the following scaling behaviour

$$\begin{aligned} \lim_{L \rightarrow \infty} S_\alpha(L/2 - x; L) &= C_\alpha \left\{ \ln \xi_e + e_\alpha + f(X) \right. \\ &\quad \left. + \xi_e^{-1/\alpha} [(-1)^x g_{\alpha,o}(Y, \varphi) + g_{\alpha,s}(Y, \varphi)] + O(\xi_e^{-2/\alpha}) \right\}, \\ \xi_e &= a_e l, \quad X \equiv x/\xi_e, \quad Y \equiv x/l^{p/(p+1)}, \end{aligned} \tag{53}$$

where e_α and a_e are constant given in equations (35) and (38) respectively. The leading spatial dependence $f(X)$ turns out to be independent of α ; it depends on p , approaching the CFT dependence $f(X) = \ln \cos(\pi X)$ with $X = x/L$ when increasing p , which is the result holding in a homogeneous chain of size L . The $O(\xi_e^{-1/\alpha})$ term presents an even-odd spatial effect proportional to $(-1)^x = e^{2ik_F x}$, scaling as a function of $Y = x/l^\zeta$ with $\zeta = p/(p+1)$, modulated by the variable φ defined in equation (31), see figures 17, 18, 19. For the harmonic potential, an accurate description of $O(\xi_e^{-1/\alpha})$ term is given by $(-1)^N b_\alpha [(-1)^x \cos(cY^3) - 1]$, see figure 20.

The above scaling behaviours have been mostly obtained by analyzing the scaling of

numerical (practically exact) results at finite trap size. Of course, it would be worthwhile to derive analytically the asymptotic trap-size dependence of the entanglement entropy, which may lead to further physical insights.

Acknowledgments

Helpful discussions with Pasquale Calabrese are gratefully acknowledged.

References

- [1] Calabrese P, Cardy J and Doyon B Eds. 2009 *Entanglement entropy in extended quantum systems*, *J. Phys. A: Math. Theor.* **42** 500301
- [2] Holzhey C, Laursen F and Wilczek F 1994 *Nucl. Phys. B* **424** 443
- [3] Vidal G, Latorre J I, Rico E and Kitaev A 2003 *Phys. Rev. Lett.* **90** 227902
- [4] Calabrese P and Cardy J 2004 *J. Stat. Mech.* P06002
- [5] Calabrese P and Cardy J 2009 *J. Phys. A: Math. Theor.* **42** 504005
- [6] Bloch I, Dalibard J and Zwerger W 2008 *Rev. Mod. Phys.* **80** 885
- [7] Greiner M, Bloch I, Mandell M O, Hänsch T and Esslinger T 2002 *Nature* **415** 39
- [8] Stöferle T, Moritz H, Schori C, Köhl M and Esslinger T 2004 *Phys. Rev. Lett.* **92** 130403
- [9] Paredes B, Widera A, Murg V, Mandel O, Fölling S, Cirac I, Shlyapnikov G, Hänsch R W and Bloch I 2004 *Nature* **429** 277
- [10] Kinoshita T, Wenger T and Weiss D S 2004 *Science* **305**, 1125
- [11] Kinoshita T, Wenger T and Weiss D S 2005 *Phys. Rev. Lett.* **95** 190406
- [12] Hadzibabic Z, Krüger P, Cheneau M, Battelier B and Dalibard J 2006 *Nature* **441** 1118
- [13] Krüger P, Hadzibabic Z and Dalibard J 2007 *Phys. Rev. Lett.* **99** 040402
- [14] Fölling S, Widera A, Müller T, Gerbier F and Bloch I 2006 *Phys. Rev. Lett.* **97** 060403
- [15] Spielman I B, Phillips W D and Porto J V 2007 *Phys. Rev. Lett.* **98** 080404
- [16] Spielman I B, Phillips W D and Porto J V 2008 *Phys. Rev. Lett.* **100** 120402
- [17] Clément D, Fabbri N, Fallani L, Fort C and Inguscio M 2009 *Phys. Rev. Lett.* **102** 155301
- [18] Jaksch D, Bruder C, Cirac J I, Gardiner C W and Zoller P 1998 *Phys. Rev. Lett.* **81** 3108
- [19] Fisher M P A, Weichmann P B, Grinstein G and Fisher D S 1989 *Phys. Rev. B* **40** 546
- [20] Campostrini M and Vicari E 2010 *Phys. Rev. A* **81** 023606
- [21] Campostrini M and Vicari E 2009 *Phys. Rev. Lett.* **102** 240601
- [22] Campostrini M and Vicari E 2010 *Phys. Rev. A* **81** 063614
- [23] Calabrese P and Lefevre A 2008 *Phys. Rev. A* **78** 032329
- [24] Peschel I 2003 *J. Phys. A: Math. Gen.* **36** L205
- [25] Latorre J I and Riera A 2009 *J. Phys. A: Math. Theor.* **42** 504002
- [26] Eisler V, Iglói F and Peschel I 2009 *J. Stat. Mech.* P02011
- [27] Sachdev S 1999 *Quantum Phase Transitions* (Cambridge Univ. Press)
- [28] Jin B-Q and Korepin V E 2004 *J. Stat. Phys.* **116** 79
- [29] Iglói F and Juhász R 2008 *Europhys. Lett.* **81** 57003
- [30] Calabrese P and Cardy J 2010 *J. Stat. Mech.* P04023
- [31] Calabrese P, Campostrini M, Essler F and Nienhuis B 2010 *Phys. Rev. Lett.* **104** 095701
- [32] Lafflorencie N, Sorensen E S, Chang M-S and Affleck I 2006 *Phys. Rev. Lett.* **96** 100603
- [33] Zhou H-Q, Barthel T, Fiaerestad J and Schollwöck U 2006 *Phys. Rev. A* **74** 050305

Scaling of bipartite entanglement in one-dimensional lattice systems with a trapping potential

Massimo Campostrini and Ettore Vicari

Dipartimento di Fisica dell'Università di Pisa and INFN, Sezione di Pisa, Largo Bruno Pontecorvo 2, I-56127 Pisa, Italy

Abstract.

We study the effects of a power-law trapping potential on the scaling behaviour of the entanglement at the quantum critical point of one-dimensional (1D) lattice particle systems. We compute bipartite von Neumann and Rényi entropies in the presence of the trap, and analyze their scaling behaviour with increasing the trap size.

As a theoretical laboratory, we consider the quantum XY chain in an external transverse field acting as a trap for the spinless fermions of its quadratic Hamiltonian representation. We then investigate confined particle systems described by the 1D Bose-Hubbard model in the superfluid phase (around the center of the trap).

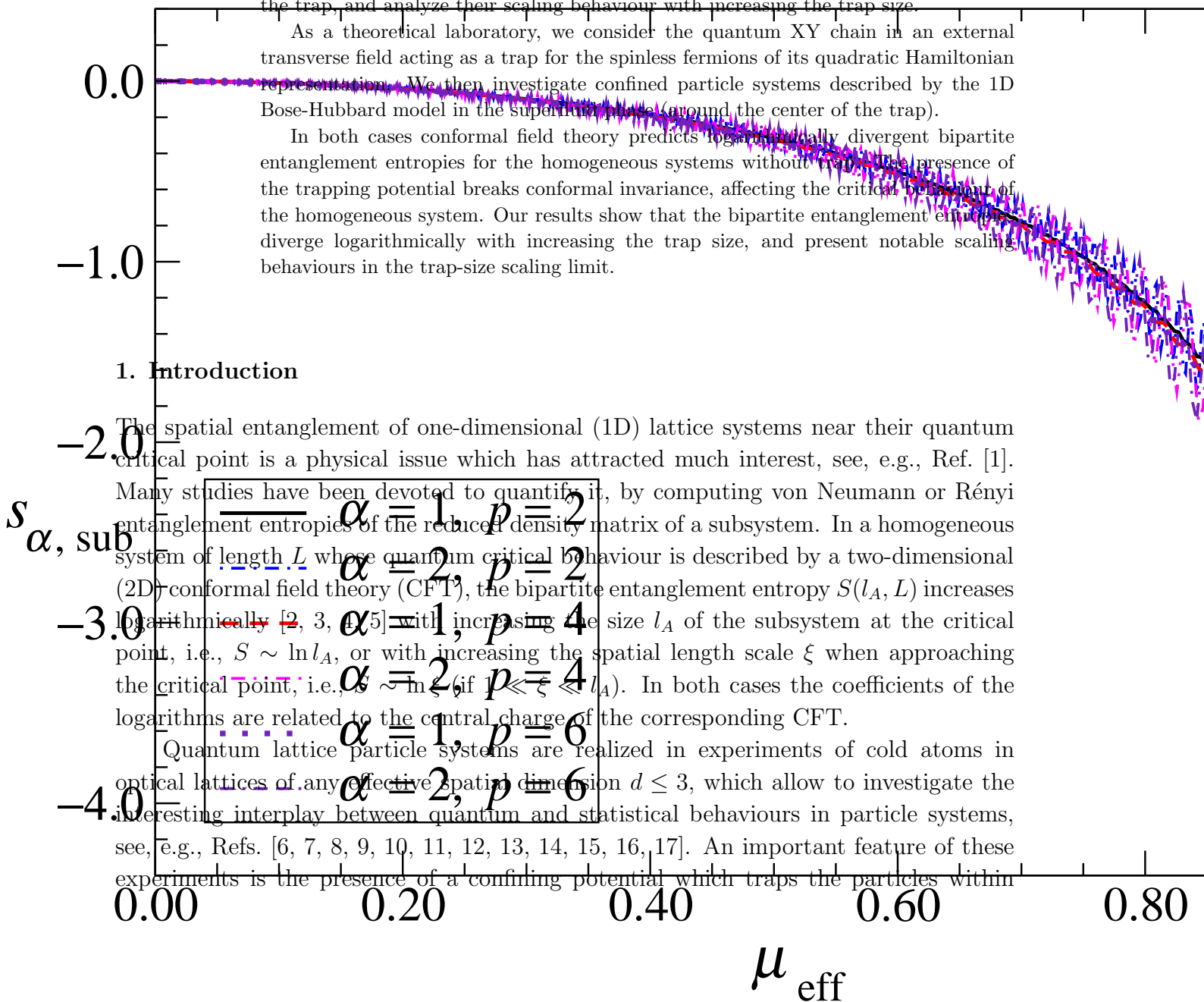
In both cases conformal field theory predicts logarithmically divergent bipartite entanglement entropies for the homogeneous systems without trap. The presence of the trapping potential breaks conformal invariance, affecting the critical behaviour of the homogeneous system. Our results show that the bipartite entanglement entropies diverge logarithmically with increasing the trap size, and present notable scaling behaviours in the trap-size scaling limit.

1. Introduction

The spatial entanglement of one-dimensional (1D) lattice systems near their quantum critical point is a physical issue which has attracted much interest, see, e.g., Ref. [1].

Many studies have been devoted to quantify it, by computing von Neumann or Rényi entanglement entropies of the reduced density matrix of a subsystem. In a homogeneous system of length L whose quantum critical behaviour is described by a two-dimensional (2D) conformal field theory (CFT), the bipartite entanglement entropy $S(l_A, L)$ increases logarithmically [2, 3, 4, 5] with increasing the size l_A of the subsystem at the critical point, i.e., $S \sim \ln l_A$, or with increasing the spatial length scale ξ when approaching the critical point, i.e., $S \sim \ln \xi$ (if $1 \ll \xi \ll l_A$). In both cases the coefficients of the logarithms are related to the central charge of the corresponding CFT.

Quantum lattice particle systems are realized in experiments of cold atoms in optical lattices of any effective spatial dimension $d \leq 3$, which allow to investigate the interesting interplay between quantum and statistical behaviours in particle systems, see, e.g., Refs. [6, 7, 8, 9, 10, 11, 12, 13, 14, 15, 16, 17]. An important feature of these experiments is the presence of a confining potential which traps the particles within



a limited spatial region of the optical lattice created by laser-induced standing waves. The theoretical framework [18] is based on the Bose-Hubbard (BH) model [19] in the presence of a confining potential coupled to the particle density, i.e.,

$$H_{\text{BH}} = -\frac{J}{2} \sum_{\langle ij \rangle} (b_i^\dagger b_j + b_j^\dagger b_i) + \frac{U}{2} \sum_i n_i(n_i - 1) + \mu \sum_i n_i + \sum_i V(r_i) n_i, \quad (1)$$

where $\langle ij \rangle$ is the set of nearest-neighbour sites, $n_i \equiv b_i^\dagger b_i$ is the particle density operator. We consider a power-law trapping potential

$$V(r) = v^p r^p \equiv (r/l)^p, \quad (2)$$

where $r \equiv |\vec{x}|$, v and p are positive constants and $l \equiv 1/v$ is the trap size. Experiments are usually set up with a harmonic potential, i.e., $p = 2$. Far from the origin the potential $V(r)$ diverges, therefore $\langle n_i \rangle$ vanishes and the particles are trapped. The inhomogeneity due to the trapping potential strongly affects the phenomenology of quantum transitions in homogeneous systems. The correlation functions develop critical behaviours only in the limit of large trap size. This critical behaviour can be described in the framework of the trap-size scaling (TSS) theory [20, 21].

In this paper we focus on the quantum entanglement in lattice particle systems confined by an external potential, such as the BH model (1). We investigate how the scaling behaviour of the entanglement entropies determined by CFT changes in the presence of the inhomogeneity induced by the confining potential.

As a theoretical laboratory we consider the quantum XY chain in an external space-dependent transverse field, acting as a trap for the spinless fermions of its quadratic Hamiltonian representation. This model presents a quantum critical behaviour belonging to the 2D Ising universality class, thus described by a CFT with central charge $c = 1/2$. In the presence of the trap and for large trap sizes, the quantum critical behaviour shows TSS [20, 21]. The presence of the trap induces a length scale ξ at the critical point, which scales nontrivially with increasing the trap size, i.e., as $\xi \sim l^\theta$ with a trap exponent $\theta = p/(p + 1)$.

We then consider the 1D BH model (1) in its hard-core limit, i.e., $U \rightarrow \infty$, and study the bipartite entanglement entropy in the gapless superfluid phase, whose continuum limit is described by a 2D massless bosonic field theory, thus a CFT with $c = 1$. In this case the trap-size dependence is made more complicated by new features [22]: (i) a multiscaling phenomenon, i.e., the existence of different length scales which diverge with distinct power laws in the TSS; (ii) the presence of level crossings of the lowest states at finite trap size, which gives rise to a peculiar modulation of the amplitudes of the asymptotic power-law behaviours.

We analyze the scaling behaviour of bipartite von Neumann and Rényi entanglement entropies in these 1D lattice models. We consider chains with even sites L and open boundary conditions, and a trap of size l centered between the middle sites of the chain. We divide the chain in two connected parts of length l_A and $L - l_A$, and consider their von Neumann entropy

$$S_1(l_A; L) = S_1(L - l_A; L) = -\text{Tr}[\rho_A \ln \rho_A] \quad (3)$$

and their Rényi entropies

$$S_\alpha(l_A; L) = S_\alpha(L - l_A; L) = \frac{1}{1 - \alpha} \ln \text{Tr} \rho_A^\alpha \quad (4)$$

where ρ_A is the reduced density matrix of one of the two subsystems. Rényi entropies are useful because they provide information on the spectrum of ρ_A [23]. The von Neumann entropy (3) is obtained by taking the limit $\alpha \rightarrow 1$ in (4). In the presence of a trap of size l , the bipartite entanglement entropies of subsystems of size $l_A = L/2 - x$ have a finite $L \rightarrow \infty$ limit, depending on x and l . We study their scaling behaviour in the large- l limit. Note that the $p \rightarrow \infty$ limit of the confining potential becomes equivalent to a homogeneous chain of size $L = 2l$ with open boundary conditions (more precisely, to a chain with even $L = 2[l]$ sites). Thus, in the $p \rightarrow \infty$ limit we must recover the entanglement entropies of homogeneous systems with open boundary conditions, which are determined by CFT.

In our numerical study we exploit the quadratic spinless fermion representations of the XY chain and the 1D hard-core BH model, which allow us to perform computations for very large systems, since they only require the diagonalization of a $L \times L$ matrix where L is the number of lattice sites. We compute the entanglement entropies using the method outlined in Refs. [24, 25], which exploits the quadratic fermionic representation and can be also applied in the presence of the trapping potential. We obtain numerical results for chains of size L and open boundary conditions, with a trap of size l centered between the middle sites of the chain; we choose L large enough to have negligible finite- L effects; we are able to obtain very accurate results for l up to $O(10^4)$.

Our results show that the bipartite entanglement entropies at the critical point diverge logarithmically with increasing the trap size. Moreover, they present notable scaling behaviours in the trap-size scaling limit.

We mention that the bipartite entanglement entropies in the XY and XX model with gradients, i.e., in the presence of a linear external field, have been recently investigated in Ref. [26].

The paper is organized as follows. In Sec. 2 we presents results for the quantum XY chain in an external space-dependent transverse field. Sec. 3 is dedicated to the 1D hard-core BH model. In Sec. 4 we draw our conclusions.

2. Bipartite entanglement in the XY chain with a space-dependent transverse field

The quantum XY chain in a transverse field is a standard theoretical laboratory for issues related to quantum transitions, see, e.g., Ref. [27]. An inhomogeneity analogous to the one arising from a trapping potential in particle systems can be achieved by considering a space-dependent transverse field, i.e.,

$$H_{\text{XY}} = - \sum_i \frac{1}{2} [(1 + \gamma) \sigma_i^x \sigma_{i+1}^x + (1 - \gamma) \sigma_i^y \sigma_{i+1}^y] - \mu \sigma_i^z - V(x_i) \sigma_i^z, \quad (5)$$

where σ^i are the Pauli matrices, $\gamma \neq 0$ and $V(x) = (|x|/l)^p$, cf. (2). The XY chain can be mapped into a quadratic Hamiltonian of spinless fermions by a Jordan-Wigner transformation, obtaining

$$\begin{aligned} H &= \sum [c_i^\dagger A_{ij} c_j + \frac{1}{2}(c_i^\dagger B_{ij} c_j^\dagger + \text{h.c.})], \\ A_{ij} &= 2\delta_{ij} - \delta_{i+1,j} - \delta_{i,j+1} + 2Q(x_i)\delta_{ij}, \\ B_{ij} &= -\gamma(\delta_{i+1,j} - \delta_{i,j+1}), \\ Q(x) &= \bar{\mu} + V(x), \quad \bar{\mu} \equiv \mu - 1. \end{aligned} \tag{6}$$

In this picture μ plays the role of *chemical potential* for the fermion *c-particles*, and the space-dependent field $V(x)$ acts as a *trap* for the *c-particles*, making their *local density* $\langle n_i \rangle \equiv \langle c_i^\dagger c_i \rangle$ vanish at large distance. In the following, l will be considered as the *trap size*.

In the absence of the trap, the model undergoes a quantum transition at $\bar{\mu} \equiv \mu - 1 = 0$ in the 2D Ising universality class, separating a quantum paramagnetic phase for $\bar{\mu} > 0$ from a quantum ferromagnetic phase for $\bar{\mu} < 0$. Around $\bar{\mu} = 0$, the quantum critical behaviour shows a diverging length scale, $\xi \sim |\bar{\mu}|^{-\nu}$, and a vanishing energy scale, $\Delta \sim \xi^{-z}$, where z and ν are universal critical exponents: $z = 1$ and $\nu \equiv 1/y_\mu = 1$ (y_μ is the RG dimension of μ).

The presence of the external field $V(x)$ gives rise to a space inhomogeneity, thus affecting the critical behaviour of the homogeneous system, which is only recovered in the limit of large trap size. In this limit the critical behaviour can be described in the framework of the trap-size scaling (TSS) theory [20]. The TSS Ansatz for the asymptotic behaviour of the free-energy density in the presence of a confining potential (2) is

$$F(\mu, T, l, x) = l^{-\theta(1+z)} \mathcal{F}(\bar{\mu} l^{\theta/\nu}, T l^{\theta z}, x l^{-\theta}), \tag{7}$$

where x is the distance from the middle of the trap, and θ is the trap-size exponent which determines how the length scale of the critical modes at the critical point diverges with increasing trap size, i.e., $\xi \sim l^\theta$. RG arguments and analytic calculations show that [20]

$$\theta = p/(p+1). \tag{8}$$

The TSS limit can be analytically derived within the quadratic spinless fermion representation (6), obtaining a Schrödinger-like equation for the lowest states, after introducing the rescaled spatial variable $X \equiv \gamma^{-\theta/p} l^{-\theta} x$, and the rescaled deviation from the critical point $\mu_r \equiv \gamma^{-\theta} l^\theta \bar{\mu}$ (see Ref. [20] for details). The γ dependence gets absorbed by such rescalings leading to a universal TSS limit. Therefore at the quantum critical point $\bar{\mu} = 0$ and $T = 0$, any length scale related to the critical modes must have the asymptotic behaviour

$$\xi = a \gamma^{\theta/p} l^\theta [1 + O(l^{-\theta})] \tag{9}$$

where the amplitude a depends on the power p of the potential, but not on γ . The power law of the scaling corrections is inferred from the analysis of the corrections to the continuum Schrödinger-like equation describing the TSS limit.

We want to study the quantum entanglement of the ground-state in the presence of the external space-dependent potential (2). For this purpose we analyze the trap-size dependence of the bipartite von Neumann and Rényi entanglement entropies, defined in equations (3) and (4), in the framework of the TSS theory.

Before presenting the results in the presence of the trap, let us recall some established results for the homogeneous XY chain with open boundary conditions, which represents the formal $p \rightarrow \infty$ limit of the model with the confining potential. They can be obtained by exploiting the CFT that describes its continuum limit. Setting

$$l_A = L/2 - x \quad (10)$$

(we consider a chain with an even number of sites L), the Rényi entropies at the critical point $\bar{\mu} = 0$ behave as [4]

$$S_\alpha(L/2 - x; L) \approx C_\alpha \left[\ln L + \ln \cos \left(\frac{\pi x}{L} \right) + e_\alpha \right] \quad (11)$$

where

$$C_\alpha \equiv c \frac{1 + \alpha^{-1}}{12} \quad (12)$$

and c is the central charge: $c = 1/2$ for the 2D Ising universality class. The constant e_α can be derived using the results of Refs. [4, 28, 29, 20], obtaining

$$e_\alpha = \ln \gamma + \ln(8/\pi) + y_\alpha, \quad (13)$$

$$y_\alpha = \int_0^\infty \frac{dt}{t} \left[\frac{6}{1 - \alpha^{-2}} \left(\frac{1}{\alpha \sinh t/\alpha} - \frac{1}{\sinh t} \right) \frac{1}{\sinh t} - e^{-2t} \right].$$

The behaviour of the von Neumann entropy can be obtained by taking the limit $\alpha \rightarrow 1$ of (11). Corrections to the asymptotic behaviour (11) are expected to be $O(L^{-1/\alpha})$ at fixed x/L [30, 31]. They become logarithmic for $\alpha \rightarrow \infty$. In the case of the von Neumann entropy, i.e., $\alpha \rightarrow 1$, corrections are $O(L^{-1})$.[‡]

In the presence of the trap of size l , the dependence on L rapidly disappears for L sufficiently larger than the trap size l . We define entanglement length scales ξ_α from the half-lattice entanglement entropies. We write (at $\bar{\mu} = 0$)

$$S_{\alpha,1/2} \equiv \lim_{L \rightarrow \infty} S_\alpha(L/2; L) \equiv C_\alpha (\ln \xi_\alpha + e_\alpha), \quad (14)$$

where e_α is the constant defined in (13). We identify the argument of the logarithm as the entanglement length scale ξ_α , which will generally depend on α and on the power p of the potential (2). However, by construction, their $p \rightarrow \infty$ limit is $\xi_\alpha \rightarrow 2l = L$ for any α . Since the entanglement length scales are clearly related to the critical modes, they are expected to have the asymptotic behaviour (9) at the critical point, although their scaling corrections may turn out to be different, depending on α .

The approach to their asymptotic behaviour $\xi_\alpha \sim l^\theta$ may be guessed by recalling that the $p \rightarrow \infty$ limit is equivalent to a homogeneous chain of size $L = 2l$ with open boundary conditions, where the corrections to the asymptotic behaviour (11) of the

[‡] It is worth mentioning that, using the relation [29] $S_\alpha(l_A; L)|_{\gamma=1} = \frac{1}{2} S_\alpha(2l_A; 2L)|_{\gamma=0}$ and results from Refs. [32, 22], we obtain $S_1(L/2; L) = \frac{1}{12} [\ln L + e_1 + (2 - 3\pi)/(4L) + O(1/L^2)]$ for $\gamma = 1$.

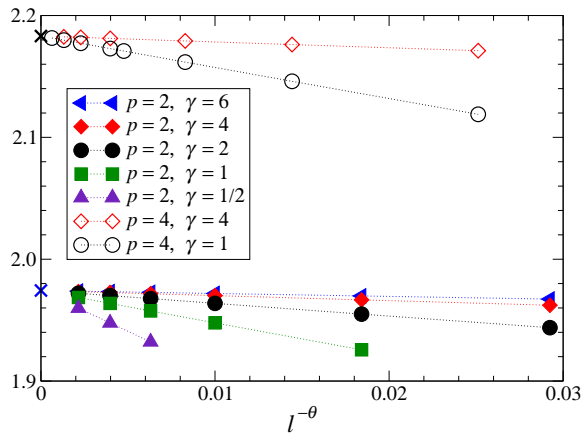


Figure 1. The ratio $\xi_1/(\gamma^{\theta/p}l^\theta)$ vs $l^{-\theta}$ for $p = 2, 4$, several values of γ , and trap sizes in the range $10^2 \leq l \leq 10^4$. The lines are drawn to guide the eyes. The crosses along the y -axis represent the γ -independent $l \rightarrow \infty$ extrapolations, see text.

Rényi entanglement entropies are [31] $O(L^{-1/\alpha})$. Then, the correspondence $L \rightarrow \xi \sim l^\theta$ suggests the presence of $O(\xi^{-1/\alpha})$, thus $O(l^{-\theta/\alpha})$, corrections. In the case of the length scale derived from the von Neumann entropy, i.e., for $\alpha \rightarrow 1$, this argument leads to the same scaling corrections of equation (9), which are expected for any length scale defined from standard correlation functions, such as $G_{ij} \equiv \langle \sigma_i^x \sigma_j^x \rangle$.

The scaling (9) is fully supported by numerical results for the half-lattice von Neumann entropy. § Figure 1 shows the results of ξ_1 for $p = 2$ and $p = 4$, several values of γ , and for trap sizes in the range $10^2 \leq l \leq 10^4$. In order to estimate the amplitude a_1 of the asymptotic behaviour

$$\xi_1 = a_1 \gamma^{\theta/p} l^\theta [1 + b_{11} l^{-\theta} + \dots], \quad (15)$$

we fit the data of the ratio $\xi_1/(\gamma^{\theta/p}l^\theta)$ to the Ansatz $a_1 + b_{1,1}l^{-\theta} + b_{1,2}l^{-2\theta}$, which turns out to be optimal, and check the stability of the results by increasing the minimum value of l allowed in the fit. The analysis of the $p = 2$ data gives $a_1 \approx 1.97431$ for all $\gamma = 6, 4, 2, 1, 1/2$,|| confirming its independence of γ , and $b_{1,1} = \bar{b}_{1,1}\gamma^{4/3}$ with $\bar{b}_{11} \approx -2.677$ independent of γ . For $p = 4$ we obtain $a_1 \approx 2.18316$ for both $\gamma = 4, 1$.

In the case of the entanglement length scales ξ_α defined from the Rényi entropies, we generally expect $\xi_\alpha \sim l^\theta$ asymptotically, with $O(l^{-\theta/\alpha})$ corrections. Assuming universality of the TSS limit, we expect that the ratios ξ_α/ξ_1 approach universal values R_α ,

$$\xi_\alpha/\xi_1 = R_\alpha + O(l^{-\theta/\alpha}) \quad (16)$$

§ The effects of the finite size L of the chain are under complete control in our numerical calculations at fixed trap size. This is easily achieved by comparing data at fixed trap size for increasing chain size, due to the fast convergence to the infinite-chain limit, see also later. We choose L large enough to have negligible finite- L effects, so that the results that we present can be effectively considered as infinite-chain results with great accuracy. Therefore, the systematic error related to the finite size of the chain is totally negligible in our analyses.

|| Here and in the following the uncertainty on the numerical estimates is at most one on the last reported figure.

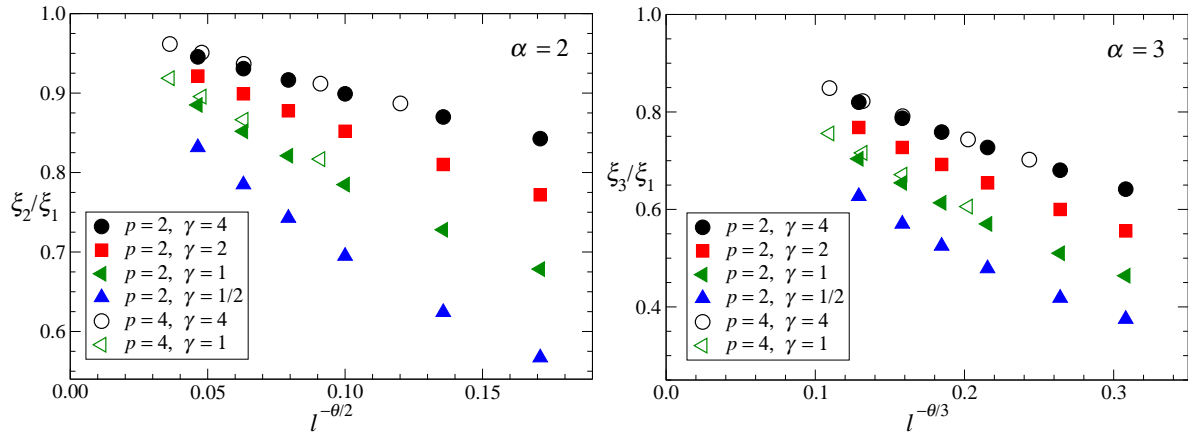


Figure 2. Ratios ξ_α/ξ_1 of entanglement length scales vs. $l^{-\theta/\alpha}$ in the presence of an external potential with $p = 2, 4$, for $\alpha = 2, 3$, several values of γ , and trap sizes in the range $10^2 \leq l \leq 10^4$.

and therefore

$$\xi_\alpha = a_\alpha \gamma^{\theta/p} l^\theta \left[1 + b_{\alpha,1}(\gamma) l^{-\theta/\alpha} + b_{\alpha,2}(\gamma) l^{-2\theta/\alpha} + \dots \right], \quad (17)$$

with a_α dependent on p but not on γ . Note that $R_\alpha \rightarrow 1$ and $a_\alpha \rightarrow 2$ for $p \rightarrow \infty$.

This scenario is confirmed by numerical results for the ratios ξ_α/ξ_1 , see figure 2 where we show results for $p = 2, 4$ and $\alpha = 2, 3$. They fit the general behaviour

$$\xi_\alpha/\xi_1 = R_\alpha + \sum_{j=1} c_j l^{-j\theta/\alpha}, \quad (18)$$

and provide consistent values of R_α for different values of γ , supporting universality. For example, we find $R_2 \approx 0.9889$, $R_3 \approx 0.987$ for $p = 2$, and $R_2 \approx 0.9970$ and $R_3 \approx 0.996$ for $p = 4$, which are slightly smaller than one, and appear to approach one with increasing p .¶

Moreover, the results for $p = 2$ indicate that the amplitudes $b_{\alpha,1}$ of the leading $O(l^{-\theta/\alpha})$ scaling corrections in equation (17) behave as $b_{\alpha,1} = \bar{b}_{\alpha,1} \gamma^{-\kappa/\alpha}$ where $\kappa = 4/3$ and $\bar{b}_{\alpha,1}$ is independent of γ , with great numerical accuracy. Analogous results are found for $p = 4$, but with $\kappa = 6/5$. Taking into account that $b_{\alpha,1} \sim \gamma^{-1/\alpha}$ for $p \rightarrow \infty$ (as inferred by numerical computations), we may guess $\kappa = (p+2)/(p+1)$. Therefore, we have that the ratios $b_{\alpha,1}^\alpha/b_{1,1}$ are independent of γ . Note that this also implies that the leading $O(l^{-\theta/\alpha})$ scaling corrections get suppressed with increasing γ for any α , including $\alpha \rightarrow 1$.

Let us now study the spatial dependence of the entanglement entropy in the presence of the trap. For this purpose we define the function

$$s_\alpha(x) \equiv C_\alpha^{-1} \lim_{L \rightarrow \infty} [S_\alpha(L/2 - x; L) - S_\alpha(L/2; L)] \quad (19)$$

¶ To get an idea of the accuracy of the universality check, we mention that, using the six available data in the range $10^2 \leq l \leq 10^4$ to fix the six parameters of the polynomial $R_\alpha + \sum_{j=1}^5 c_j e^{-j\theta/\alpha}$, we obtain $R_2 = 0.98892, 0.98892, 0.98892, 0.98889$ and $R_3 = 0.9867, 0.9867, 0.9868, 0.9869$ for $\gamma = 4, 2, 1, 1/2$ respectively.

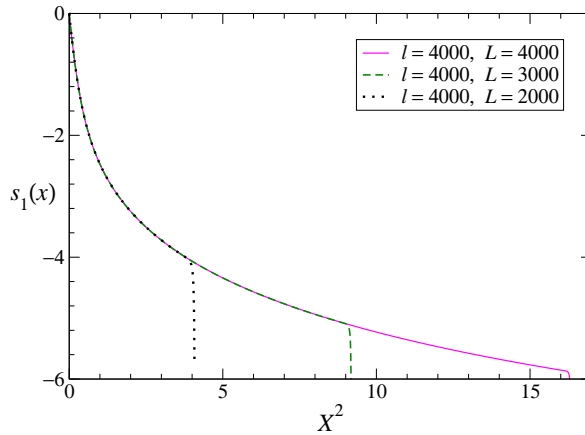


Figure 3. $s_1(x)$, cf. (19), vs. X^2 , for $\gamma = 1$, $p = 2$, $l = 4000$ and a few values of the size of the chain L .

This limit is finite and depends only on x and the trap size l . We expect that in the TSS limit

$$s_\alpha(x) \approx f_\alpha(X), \quad X \equiv x/\xi_1, \quad (20)$$

i.e., they are scaling functions of X . Note that the distance of the site $L/2 - x$ from the center of the trap is actually $y = x + 1/2$, but the effects of this difference disappears in the TSS limit $\xi_1 \rightarrow \infty$ at fixed $X \equiv y/\xi_1$, as $O(\xi_1^{-1})$. The large- p limits of f_α coincide, indeed, since $\xi_1 \rightarrow L$, (11) implies

$$\lim_{p \rightarrow \infty} f_\alpha(X) = \ln \cos(\pi X) \quad (21)$$

with $|X| < 1/2$. Corrections to scaling are again expected to be $O(l^{-\theta/\alpha})$.

In figure 3 we show data for $p = 2$, $\gamma = 1$, $l = 4000$ and a few values of the size of the chain L . They show the effects of the finite size L of the chain, and that accurate results for larger and larger X require larger and larger L . However, such effects can be carefully controlled, so that the results that we will present can be effectively considered as infinite-chain results. ⁺ We used chains of size up to $L = 4000$ for $\gamma = 1$ and up to $L = 6000$ for $\gamma = 4$, which ensure negligible finite- L effects at the trap size considered.

The numerical results for the von Neumann entropy, reported in figure 4 for $p = 2$ and $p = 4$, show that $s_1(x)$ approaches a scaling function of $X \equiv x/\xi_1$ in the TSS limit (more precisely, a function of X^2 , since it is an even function of X), which is universal, i.e., independent of γ . In figure 4 we also show extrapolations to $l \rightarrow \infty$ assuming $O(l^{-\theta})$ corrections. They are consistent with a universal TSS limit independent of γ . With

⁺ The comparison of data in Fig. 3 shows that we can obtain very accurate results around the middle of the trap even without requiring $l \ll L$, as one might naively expect. This is essentially related to the fact that the relevant length scale of the critical correlations behaves as $\xi \sim l^\theta$ and $\theta < 1$, so that we can have $\xi \ll L$ even when $l \approx L$. Note that, with increasing the power p of the confining potential, θ increases and approaches one, thus larger chain sizes are required at fixed trap size (we recall that for $p \rightarrow \infty$ we have the formal correspondence $L = 2l$).

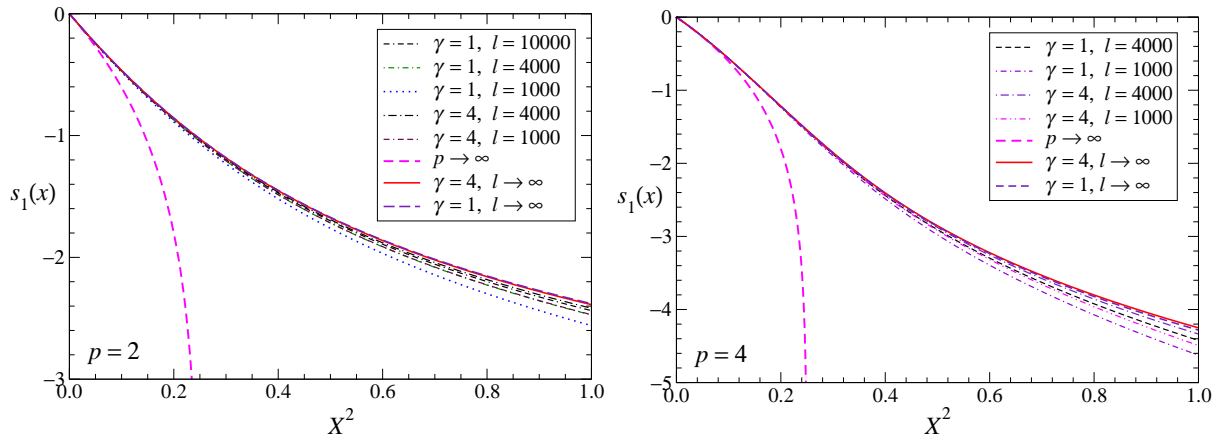


Figure 4. The function $s_1(x)$, cf. (19), vs. X^2 , for $p = 2, 4$, $\gamma = 1, 4$, and a few values of l . Curves for $l \rightarrow \infty$ are obtained by using the data for the three largest values of l , extrapolating at fixed X using the second-order polynomial $\sum_{n=0}^2 c_n l^{-n\theta}$. The extrapolated curves of data at $\gamma = 1, 4$ can be hardly distinguished, supporting the universality of the TSS. For comparison we also show the $p \rightarrow \infty$ limit (21).

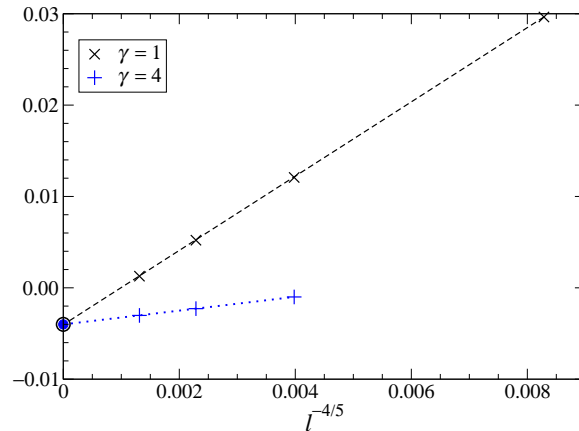


Figure 5. Results for $c_2 - c_2|_{p \rightarrow \infty} = c_2 + \pi^2/2$, cf. (22), for $p = 4$, using data for $\gamma = 1, 4$, versus $l^{-\theta}$. The crosses indicate the estimates of c_2 from polynomial fits of $s_1(x)$ at small x , which are expected to converge to its $l \rightarrow \infty$ with $O(l^{-\theta})$ corrections. The lines show linear fits of these data to $c_2 + a_\gamma l^{-\theta}$. The blobs along the y -axis show the estimates of c_2 from the fits of the $l \rightarrow \infty$ extrapolated curves of $s_1(x)$ for $\gamma = 1, 4$. The overall agreement with a universal value of c_2 is very accurate, leading to the estimate $c_2 - c_2|_{p \rightarrow \infty} \approx -0.0040$.

increasing p , the curves approach the $p \rightarrow \infty$ limit (21). The approach is particularly fast at small X , where we find

$$f_1(X) = c_2 X^2 + O(X^4) \quad (22)$$

with $c_2 \approx -4.988$ for $p = 2$ and $c_2 \approx -4.939$ for $p = 4$ (see figure 5), to be compared with $c_2 = -\pi^2/2 \approx -4.93480$ for $p \rightarrow \infty$, obtained by expanding equation (21).

Analogous results are obtained from the Rényi entropies, see figures 6 and 7, respectively for $\alpha = 2$ and $\alpha = 3$. In these cases the approach to the large- l limit is slower, because corrections are $O(l^{-\theta/\alpha})$. As a consequence the $l \rightarrow \infty$ extrapolations

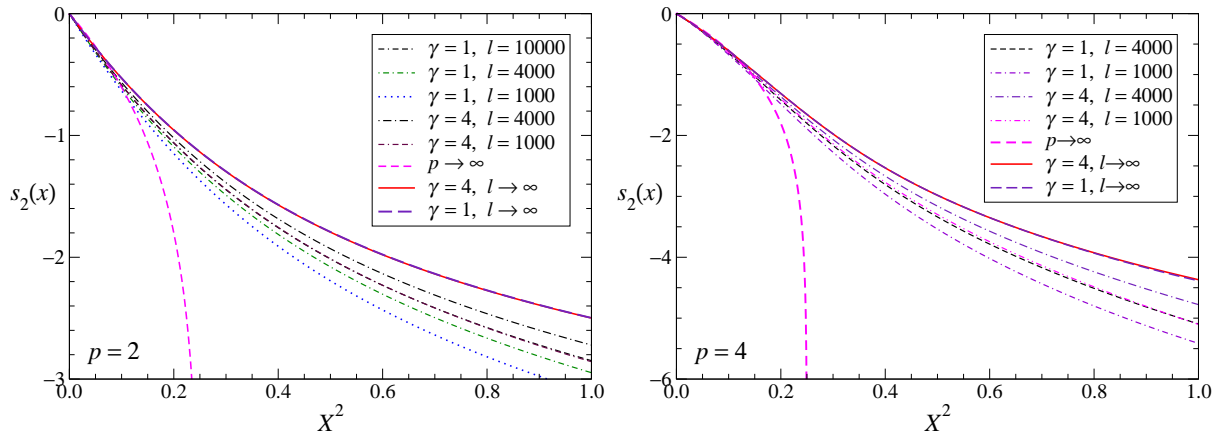


Figure 6. The function $s_2(x)$, cf. (19), vs. X^2 , for $p = 2, 4$, $\gamma = 1, 4$, and a few values of l . Curves for $l \rightarrow \infty$ are obtained by using the data for the three largest values of l , extrapolating at fixed X using the second-order polynomial $\sum_{n=0}^2 c_n l^{-n\theta/2}$. The extrapolated curves of data at $\gamma = 1, 4$ can be hardly distinguished, supporting the universality of the TSS. For comparison we also show the $p \rightarrow \infty$ limit (21).

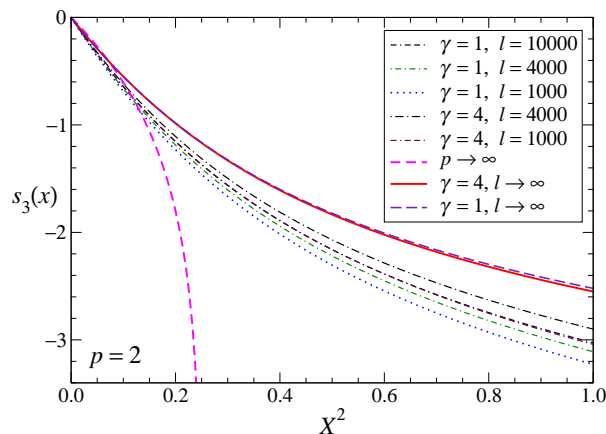


Figure 7. The function $s_3(x)$, cf. (19), vs. X^2 , for $p = 2$, $\gamma = 1, 4$, and a few values of l . Curves for $l \rightarrow \infty$ are obtained by using the data for the largest values of l , extrapolating at fixed X using the polynomials $\sum_{n=0}^{\bar{n}} c_n l^{-n\theta/3}$ with $\bar{n} = 2$ for $\gamma = 4$ and $\bar{n} = 3$ for $\gamma = 1$. For comparison we also show the $p \rightarrow \infty$ limit (21).

tend to be more imprecise with increasing α , see indeed the case $\alpha = 3$ in figure 7. Larger values of α would require larger trap sizes to get reliable $l \rightarrow \infty$ extrapolations, due to the slowly decaying $O(l^{-\theta/\alpha})$ scaling corrections. Comparing the results for $\alpha = 1, 2, 3$, we see that the functions $f_\alpha(X)$ turn out to depend little on α .

3. The 1D hard-core Bose-Hubbard model with a trapping potential

We now consider the 1D Bose-Hubbard (BH) model (1), which is of experimental relevance because it describes quasi-one-dimensional cold atoms in optical lattices, see, e.g., Refs. [6, 9, 10, 11, 17]. We consider its hard-core limit $U \rightarrow \infty$, which implies that the particle number is restricted to the values $n_i = 0, 1$, and allows us to study the

effects of the confining potential by very accurate numerical results.

The hard-core limit of the 1D BH model can be mapped into the XX chain model with a space-dependent transverse external field,

$$H_{\text{XX}} = -\frac{J}{4} \sum_i (\sigma_i^x \sigma_{i+1}^x + \sigma_i^y \sigma_{i+1}^y) - \frac{1}{2} \sum_i [\mu + V(x_i)] \sigma_i^z, \quad (23)$$

(which is the Hamiltonian (5) with $\gamma = 0$, apart from a factor 2). The Pauli spin matrices are related to the boson operators of the BH Hamiltonian H_{BH} , cf. (1), by $\sigma_i^x = b_i^\dagger + b_i$, $\sigma_i^y = i(b_i^\dagger - b_i)$, $\sigma_i^z = 1 - 2b_i^\dagger b_i$. One can then map the XX chain into a model of free spinless fermions by a Jordan-Wigner transformation, given by (6) for $\gamma = 0$ (apart from a factor 2).

In the absence of the trap, the 1D hard-core BH model has three phases: two Mott insulator phases, for $\mu > 1$ with $\langle n_i \rangle = 0$ (empty state) and for $\mu < -1$ with $\langle n_i \rangle = 1$, separated by a gapless superfluid phase for $|\mu| < 1$ characterized by the filling factor

$$f \equiv \langle n_i \rangle = (1/\pi) \arccos \mu. \quad (24)$$

A general analysis of the trap-size dependence and TSS at the Mott transitions and within the superfluid phase of the hard-core BH model (1) has been presented in Ref. [22]. Here we focus on the behaviour of the quantum entanglement within the superfluid phase, i.e., for $|\mu| < 1$, whose continuum limit is described by a free massless bosonic field theory with dynamic exponent $z = 1$, thus a conformal field theory with $c = 1$. Specifically, we consider the model at $\mu = 0$, corresponding to half filling in the absence of the trap.

3.1. Modulated multi-TSS in the superfluid phase

The trap-size dependence shows subtle effects in the parameter region where the homogeneous model without trap has a nonzero filling f , i.e., for $\mu < 1$, including the superfluid phase. This is essentially related to the presence of level crossings of the lowest states at finite trap size. They arise because the particle number is conserved, i.e., the particle number operator $\hat{N} = \sum_i n_i$ commutes with the BH Hamiltonian (1) even in the presence of the trapping potential; thus the eigenvectors do not depend on μ , even though the eigenvalues do. In the presence of the trapping potential (2), the particle number $N \equiv \langle \hat{N} \rangle$ is finite and increases as $N \sim l$ with increasing the trap size l , see (29). Therefore, as $l \rightarrow \infty$, there is an infinite number of ground-state level crossings where N jumps by 1 and the gap vanishes. In spite of the presence of these level crossings, the length scale of the critical modes diverges only in the large trap-size limit. Note that the hard-core limit, $U \rightarrow \infty$ in (1), or the spatial dimension do not play any special role, so we expect that level crossings at finite trap size are a general feature of the BH model (1) in the presence of a confining potential, when the homogeneous limit of infinite trap size has a finite particle density. The main effect of the infinite level crossings in the limit $l \rightarrow \infty$ is that the asymptotic power law behaviours get modulated by periodic functions of the trap size l , giving rise to a modulated TSS.

Moreover, in the superfluid region, the scaling of the spatial dependence of the correlation functions is characterized by two independent length scales having different power-law divergences in the large trap-size limit. One of them scales as

$$\xi_s \sim l \quad (25)$$

and describes the behaviour of observables related to smooth modes, such as the gap and the half-lattice entanglement entropy; the other one scales as

$$\xi_F \sim l^\zeta, \quad \zeta = p/(p+1), \quad (26)$$

and it is found in observables involving the modes at the Fermi scale $k_F = \pi f$, such as the density-density correlation. This gives rise to a multi-TSS behaviour, which is more complicated than that described by the scaling Ansatz (7) which applies to the XY chain model around its quantum critical point.

As we shall see, the behaviour of the quantum entanglement of parts of the system in its ground state reflects the above general features.

In the following we briefly mention a number of results obtained in Ref. [22] which will be useful for the discussion of the quantum entanglement.

The particle density of the 1D hard-core BH model approaches its local density approximation (LDA) in the large- l limit, i.e., the value of the particle density of the homogeneous system at the effective chemical potential

$$\mu_{\text{eff}}(x) \equiv \mu + (x/l)^p. \quad (27)$$

The LDA of the particle density reads

$$\langle n_x \rangle_{\text{lda}} \equiv \rho_{\text{lda}}(x/l) = \begin{cases} 0 & \text{for } \mu_{\text{eff}}(x) > 1, \\ (1/\pi) \arccos \mu_{\text{eff}}(x) & \text{for } -1 \leq \mu_{\text{eff}}(x) \leq 1, \\ 1 & \text{for } \mu_{\text{eff}}(x) < -1. \end{cases} \quad (28)$$

Corrections are generally suppressed by powers of the trap size, and present a nontrivial scaling behaviour [22] in term of the scaling variable $Y \equiv x/l^\zeta$.

Asymptotically, the total particle number is obtained by integrating the local density approximation of the particle density ρ_{lda} :

$$N \equiv \langle \hat{N} \rangle = c_\mu l + O(1), \quad c_\mu = 2 \int_0^\infty \rho_{\text{lda}}(y) dy. \quad (29)$$

At $\mu = 0$ we have $c_{\mu=0} \approx 0.76276$ for $p = 2$, $c_{\mu=0} \approx 0.859407$ for $p = 4$, and $c_{\mu=0} \rightarrow 1$ for $p \rightarrow \infty$.

In the superfluid region the interval between subsequent level crossings $l_0^{(k)}$ (where k enumerates them with increasing trap size) tends to a constant value in the large trap-size limit, given by [22]

$$\lim_{k \rightarrow \infty} \left(l_0^{(k+1)} - l_0^{(k)} \right) = 1/c_\mu, \quad (30)$$

with $O(l^{-2})$ corrections (this formula has been checked with great accuracy by numerical computations). In the limit $p \rightarrow \infty$ the interval of level crossings converges toward the

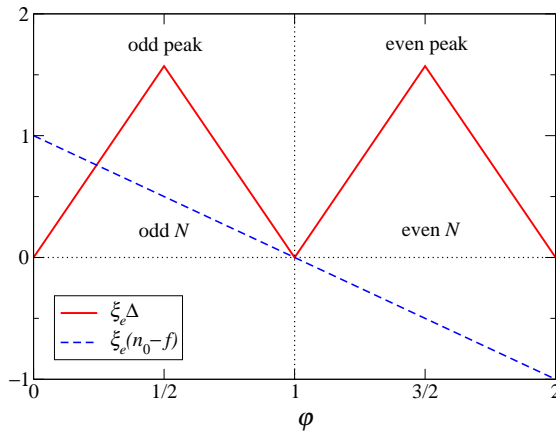


Figure 8. The asymptotic behaviour of the gap and the particle density at the center of the trap at $\mu = 0$, thus $f = 1/2$. In formulae [22], $\Delta = \pi t(\varphi)/\xi_e$ and $\langle n_0 \rangle - f = (1 - \varphi)/\xi_e$, where ξ_e is the entanglement length scale defined in (38). These results apply for any p , including $p \rightarrow \infty$.

corresponding value in the finite-size behaviour of the homogeneous system with open boundary conditions, which is $1/(2f)$.

The amplitudes of the asymptotic power law behaviours turn out to be modulated by periodic functions of the trap size, whose period is related to the level crossing interval (30). In order to describe such phenomenon, since some quantities distinguish between odd and even level crossings, we introduce the phase-like variable

$$\varphi = 2 \frac{l - l_0^{(2k)}}{l_0^{(2k+2)} - l_0^{(2k)}} \quad \text{for } l_0^{(2k)} \leq l < l_0^{(2k+2)}, \quad (31)$$

thus $0 \leq \varphi < 2$. φ provides the normalized distance from the largest even level crossing smaller than the given l .^{*} Values in the range $0 \leq \varphi \leq 1$ corresponds to ground states with odd particle numbers, while the range $1 \leq \varphi \leq 2$ corresponds to even particle numbers. Note that (30) implies that φ is a periodic function of l in the asymptotic regime.

In the superfluid phase, i.e. $|\mu| < 1$, the asymptotic behaviours of the gap and the particle density at the center of the trap are given by

$$\begin{aligned} \Delta &\sim t(\varphi)l^{-1}, & t(\varphi) &= 1/2 - ||1 - \varphi| - 1/2|, \\ \langle n_0 \rangle - f &\sim (1 - \varphi)l^{-1}, \end{aligned} \quad (32)$$

respectively. The amplitudes of the asymptotic power-law behaviours get modulated by periodic functions of the trap size, through the dependence of φ of their amplitudes. The values $\varphi = 1/2$ and $\varphi = 3/2$ correspond to the odd and even peaks of the gap, where the particle number $N = \langle \hat{N} \rangle$ is odd and even respectively. In figure 8 we show their behaviours at $\mu = 0$.

An analogous modulation of the asymptotic behaviours is found in the limit $p \rightarrow \infty$, i.e. for a homogeneous chain of size L with open boundary conditions [22]. In this case,

^{*} In Ref. [22] the variable φ was denoted by $\bar{\phi}$.

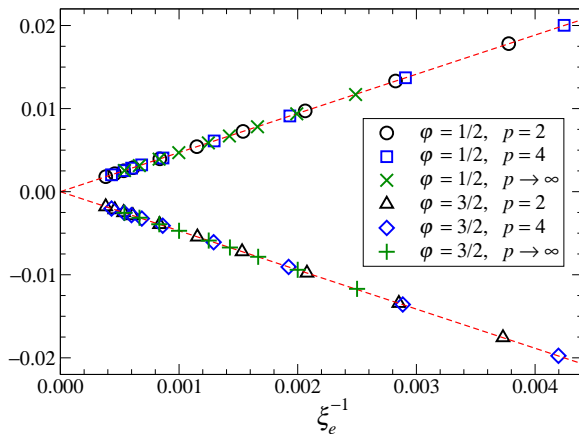


Figure 9. The quantity $\xi_e(6S_{1,1/2} - \ln \xi_e - e_1)$, for $\varphi = 1/2, 3/2$ and $p = 2, 4, \infty$. The dashed lines show the linear behaviour $\pm 3\pi/(2\xi_e)$ for $\varphi = 1 \mp 1/2$, in agreement with (37).

the variable φ reads

$$\varphi \equiv 2\{[(L+1)f + 1]/2\}, \quad (33)$$

where $\{x\} \equiv x - [x]$ is the fractional part of x (i.e., the sawtooth function). The asymptotic behaviour of the gap is given by

$$\Delta = \pi(1 - \mu^2)^{1/2} t(\varphi) L^{-1}. \quad (34)$$

At $\mu = 0$, i.e., $f = 1/2$, the variable φ takes only discrete values: $\varphi = 0, 1/2, 1, 3/2$ (the values $1/2$ and $3/2$ corresponds to even chain size, with odd and even particle number respectively).

3.2. Asymptotic trap-size dependence of the bipartite entanglement entropies

Let us consider a chain with even L sites and open boundary conditions, and a trap of size l centered between the middle sites of the chain. We again divide it into two subsystems and study the behaviours of the von Neumann and Rényi entropies of one of the subsystems. We present results up to trap sizes $l = O(10^3)$, corresponding to total particle numbers of $O(10^3)$, see equation (29). We used chains of size up to $L = 3000$ to achieve negligible finite- L effects (a more detailed discussion of this point for the XX chain can be found in the App. A of Ref. [22]).

In the absence of the trap, the behaviour of the entanglement entropies is given by (11) with $c = 1$, with

$$e_\alpha = \ln \sqrt{1 - \mu^2} + \ln(4/\pi) + y_\alpha, \quad (35)$$

obtained using the results of Refs. [4, 28, 29]. Corrections are again expected to be $O(L^{-1/\alpha})$ [31, 30]. The large- L behaviour of numerical results is indeed compatible with

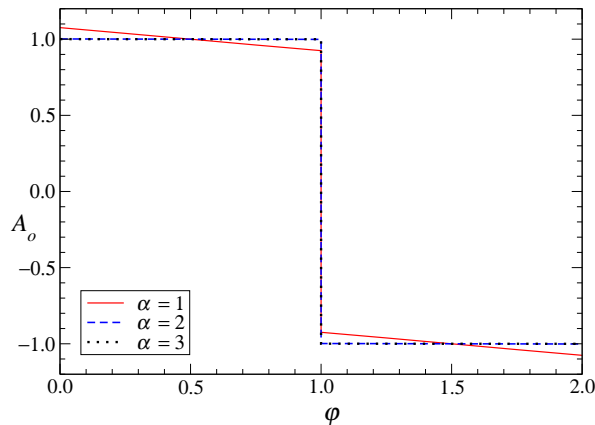


Figure 10. The function $A_o(\varphi)$ as obtained from data at $l \approx 998$, normalized so that $A_o(1/2) = 1$ and $A_o(3/2) = -1$.

the following asymptotic behaviour

$$S_\alpha(L/2 - x; L) = C_\alpha \left[\ln(L+1) + \ln \cos(\pi X) + e_\alpha - (-1)^{L/2-x} \frac{b_\alpha}{(L \cos \pi X)^{1/\alpha}} + O(L^{-2/\alpha}) \right] \quad (36)$$

with $X \equiv x/(L+1)$, and $b_1 = 3\pi/2 \approx 4.71239$, $b_2 \approx 4.79256$ and $b_3 \approx 4.19726$. Note that the factor $L+1$ in the logarithm and in the definition of X is essential to get a formula which is correct up to $O(L^{-2})$ at fixed X in the case of the von Neumann entropy ($\alpha = 1$).

The half-lattice von Neumann entropy in the presence of the trap was already considered and numerically investigated in Ref. [22], finding an entanglement length scale which increases linearly with the trap size in the whole superfluid region. Specifically, at $\mu = 0$ and for any power p of the potential, including $p \rightarrow \infty$, the half-lattice von Neumann entropy behaves as [22]

$$S_{1,1/2} = \frac{1}{6} \left[\ln \xi_e + e_1 + A_o(\varphi) \frac{3\pi}{2\xi_e} + O(\xi_e^{-2}) \right], \quad (37)$$

where

$$\xi_e = a_e l, \quad a_e = \sqrt{\pi} \Gamma\left(\frac{1}{2p}\right) \left[p \Gamma\left(\frac{1+p}{2p}\right) \right]^{-1}. \quad (38)$$

ξ_e provides an entanglement length scale, and $A_o(\varphi)$ is a periodic function of l which can be parametrized by

$$A_o(\varphi) = \begin{cases} 1 + q(\varphi - 1/2) & \text{for } 0 < \varphi < 1, \\ -1 - q(3/2 - \varphi) & \text{for } 1 < \varphi < 2 \end{cases} \quad (39)$$

Note that $A_o(1 \mp 1/2) = \pm 1$. In figure 9 we show results for $p = 2, 4, \infty$ and $\varphi = 1/2, 3/2$. They clearly support equation (37). The function $A_o(\varphi)$ is shown in figure 10 for $p = 2$ for trap sizes around $l \approx 998$. We estimate $q \approx -0.152$ for $p = 2$ and $q \approx -0.044$ for $p = 4$. The parametrization (39) of $A_o(\varphi)$ is convenient when

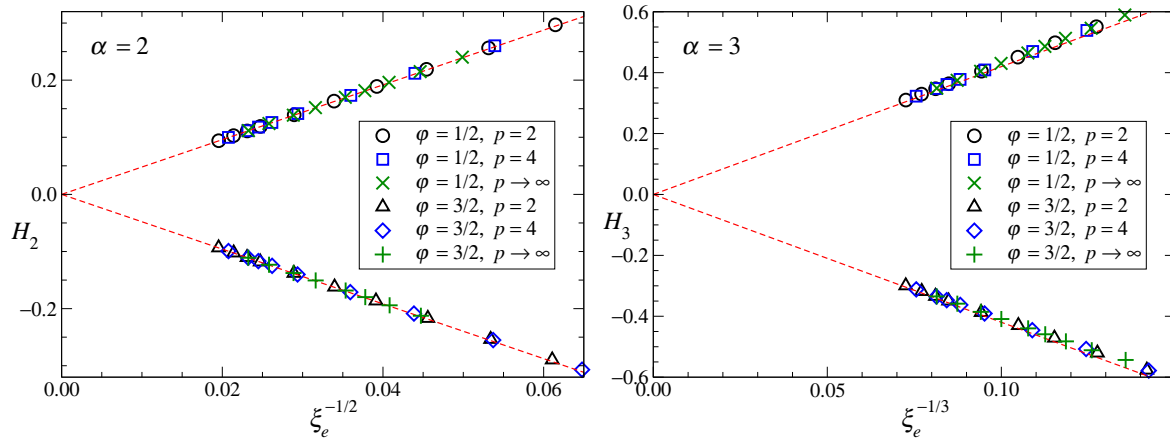


Figure 11. The quantity H_α , defined in (40), for $\alpha = 2, 3$, $\varphi = 1/2, 3/2$ and $p = 2, 4, \infty$. The dashed lines show the linear behaviour $\pm b_\alpha \xi_e^{-1/\alpha}$ for $\varphi = 1 \mp 1/2$, with $b_2 = 4.79256$ and $b_3 = 4.19726$, cf. (41).

comparing with the $p \rightarrow \infty$ limit, because $\varphi = 1/2, 3/2$ are the only possible values for the homogeneous system in a chain with even L , corresponding to odd and even $L/2$ (thus odd and even particle number N) respectively. The behaviour of the homogeneous system with open boundary condition, cf. (11), is obtained by replacing $\xi_e \rightarrow L + 1$ at the values $\varphi = 1/2, 3/2$.

We now show that the half-lattice Rényi entropies show analogous behaviours. In figure 11 we show numerical results of the quantity

$$H_\alpha \equiv \xi_e^{1/\alpha} (C_\alpha^{-1} S_{\alpha,1/2} - \ln \xi_e - e_\alpha) \quad (40)$$

for $p = 2, 4, \infty$ and $\varphi = 1/2, 3/2$. The data appears to follow curves which are apparently independent of p , but clearly depending on φ . Therefore, analogously to the case of the von Neumann entropy, the asymptotic behaviour of the Rényi entropies show the same form for any value of the potential power p , including $p \rightarrow \infty$, when they are expressed in terms of the entanglement length scale ξ_e , i.e.,

$$S_{\alpha,1/2} = C_\alpha [\ln \xi_e + e_\alpha + b_\alpha A_{\alpha,o}(\varphi) \xi_e^{-1/\alpha} + O(\xi_e^{-2/\alpha})] \quad (41)$$

where b_α are the same constants entering the behaviour of the half-lattice Rényi entanglement entropies of the homogeneous system, cf. (36), and $A_{\alpha,o}$ is given by (39), with very small values of q , i.e. $q \approx -0.003$ for $\alpha = 2, p = 2$ and $q \approx -0.001$ for $\alpha = 3, p = 2$. Thus $A_{\alpha,o} \approx (-1)^N$ for $\alpha > 1$. Equations (37) and (41) imply that the length scales defined in (14) behave as

$$\xi_\alpha = \xi_e [1 + O(\xi_e^{-1/\alpha})] \quad (42)$$

for any α .

We now analyze the spatial dependence of the bipartite entanglement entropies. We again consider the functions defined in (19). In figures 12, 13, and 14 we show results for $p = 2, 4, \alpha = 1, 2, 3, \varphi = 1/2, 3/2$, and several values of the trap size. In all cases the behaviours of the functions $s_\alpha(x)$, defined as in (19), are characterized by a

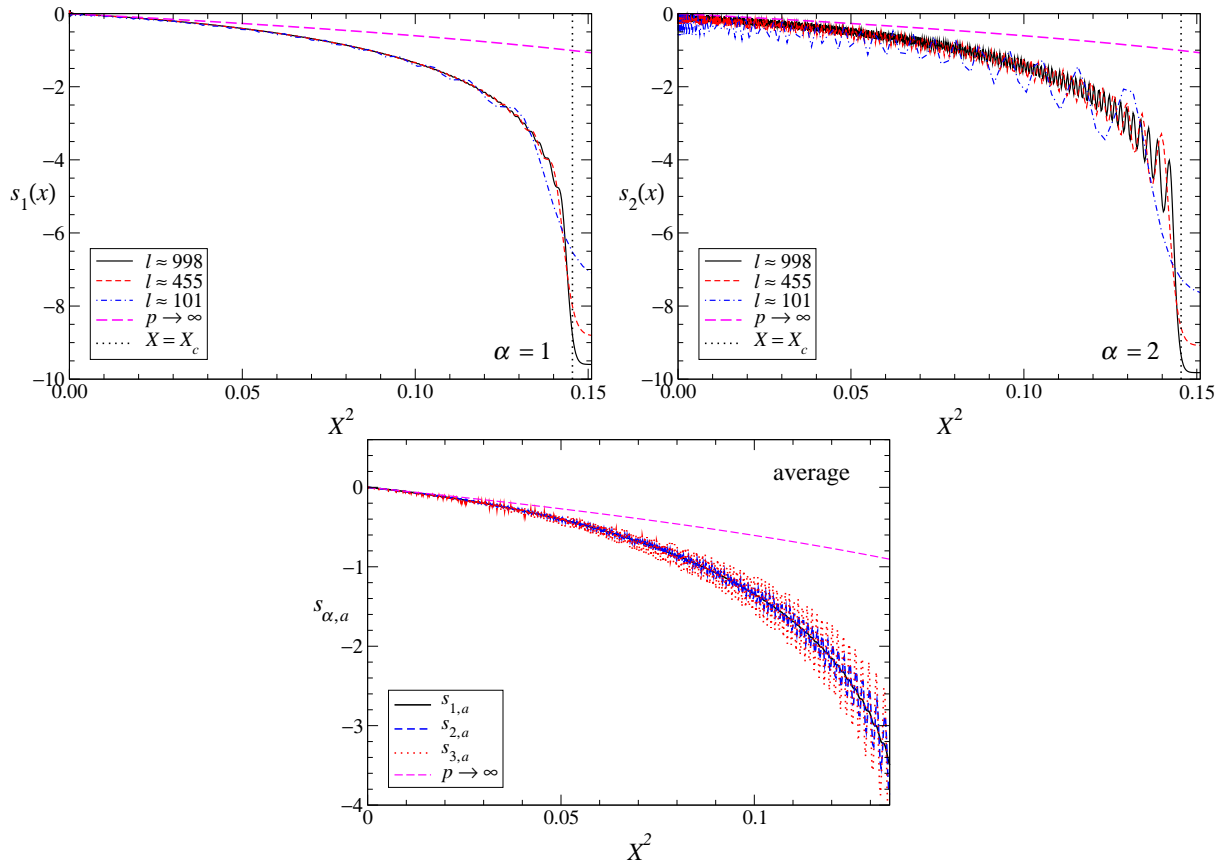


Figure 12. s_α vs. X^2 , for $\alpha = 1, 2, 3$, $p = 2$, $\varphi = 1/2$, and a few values of l . The vertical dotted lines show the value $X = X_c = 1/a_e$, cf. (38).

smooth function $f_\alpha(X)$ with $X \equiv x/\xi_e$, and oscillations around it, which appear larger and larger with increasing α , but get suppressed with increasing ξ_e . These numerical results suggest

$$s_\alpha(x) = f_\alpha(X) + O(\xi_e^{-1/\alpha}), \quad X \equiv x/\xi_e, \quad (43)$$

where the power-law of the corrections can be guessed from the fact that $O(L^{-1/\alpha})$ corrections are expected in homogeneous system with open boundary conditions [31, 30]. Moreover, the numerical results strongly suggest that a unique function describes the leading behaviour for any α , i.e., $f_\alpha(X) \equiv f(X)$ is independent of α , for any p . This becomes more evident when considering the average $s_{\alpha,a}$ of the functions $s_\alpha(x)$ at subsequent odd and even peaks of the gap (indeed, as we shall see below, the curves at $\varphi = 1/2$ and $\varphi = 3/2$ have opposite oscillating corrections at least for sufficiently small values of X). With increasing p the function $f(X)$ appears to tend to the $p \rightarrow \infty$ limit given by (21). Actually, the small- X behaviour at $p = 2$ is already very close to the $p \rightarrow \infty$ limit (the large- l extrapolation of the coefficient c_2 of the $O(X^2)$ term is compatible with its $p \rightarrow \infty$ limit $c_2 = -\pi^2/2$ already at $p = 2, 4$). On the other hand, oscillations are strongly dependent on α .

An interesting numerical relation concerning the leading behaviour $f(X)$ is illustrated in figure 15: for $p = 2, 4, 6$, we find that the difference between $f(X)$

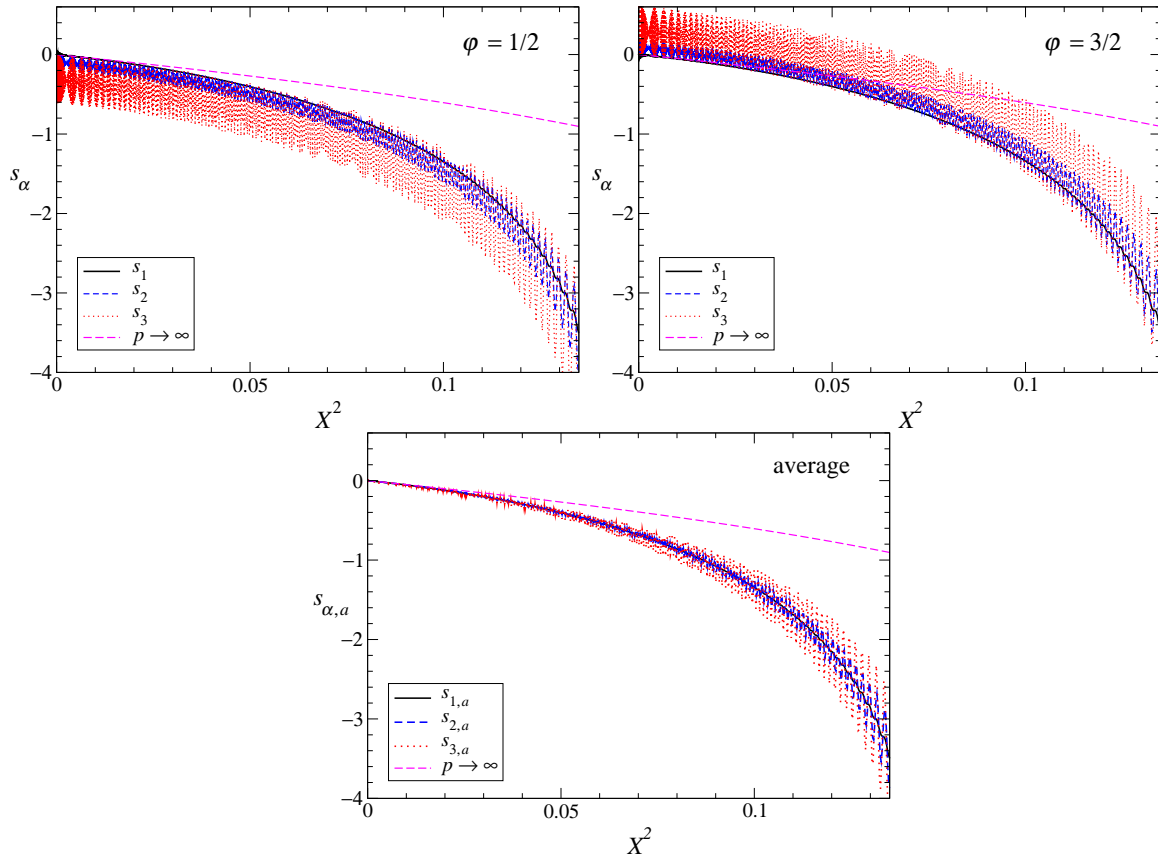


Figure 13. s_α vs. X^2 for $\alpha = 1, 2, 3$, $p = 2$, and $l \approx 10^3$, at $\varphi = 1/2$, $\varphi = 3/2$, corresponding to $N = 761, 762$, and their average $s_{\alpha,a} \equiv (s_\alpha|_{\varphi=1/2} + s_\alpha|_{\varphi=1/3})/2$, which has much smaller oscillations.

and its $p \rightarrow \infty$ limit given by CFT, i.e. $\lim_{p \rightarrow \infty} f(X) = \ln \cos \pi X$, is a function of $\mu_{\text{eff}} \equiv (|x|/l)^p = (a_e X)^p$ only, i.e.,

$$f(X) \approx \ln \cos \pi X + A(\mu_{\text{eff}}) \quad (44)$$

where the (p -independent) function A behaves as $A(\mu_{\text{eff}}) = O(\mu_{\text{eff}}^2)$ at small X (more precisely the numerical results indicate $A(\mu_{\text{eff}}) = a\mu_{\text{eff}}^2 + O(\mu_{\text{eff}}^4)$ with $a \approx -1.0$).

Note that the von Neumann and Rényi entropies rapidly decrease around $X = X_c$ corresponding to $x_c \equiv l$, thus $X_c = 1/a_e$, cf. (38); x_c is the value of x where $\mu_{\text{eff}}(x) = (x/l)^p = 1$, i.e., the value of the chemical potential corresponding to the superfluid to empty state transition, where the particle density of the ground state vanishes, see equation (28). We thus expect that, for generic values of μ and p , the region around $x = x_c$ develops critical modes related to a low-density Mott transition from the superfluid phase to the empty state. The effective chemical potential can be expanded around x_c as

$$\mu_{\text{eff}} = (x/l)^p = 1 + p \frac{x - x_c}{l} + O[(x - x_c)^2]. \quad (45)$$

Thus, the behaviour around x_c is essentially analogous to that arising at the low-density Mott transition $\mu = 1$ in the presence of a linear potential $V_l \sim r/l$. Around x_c , critical

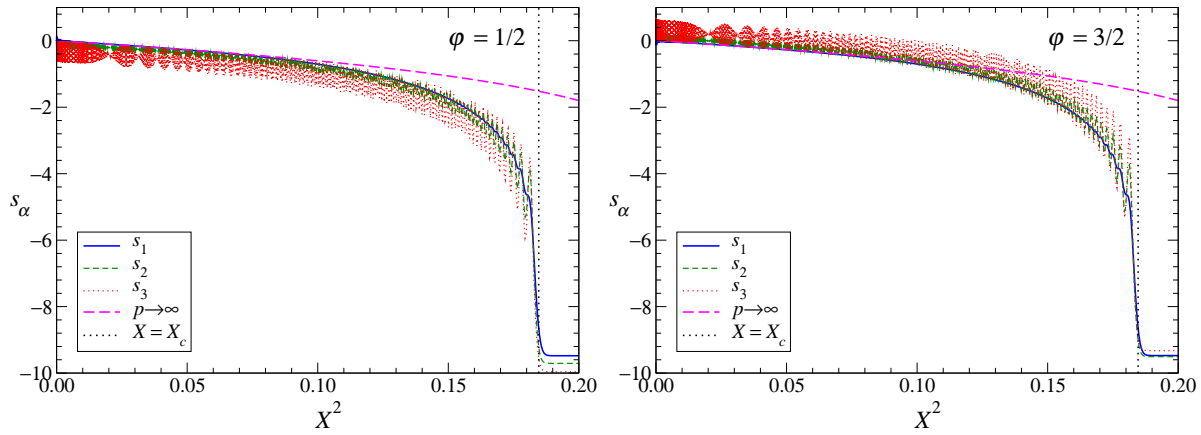


Figure 14. s_α vs. X^2 for $\alpha = 1, 2, 3$, $p = 4$, $l \approx 10^3$, and $\varphi = 1/2, 3/2$, corresponding to $N = 857, 856$. The vertical dotted lines show the value $X = X_c = 1/a_e$, cf. (38).

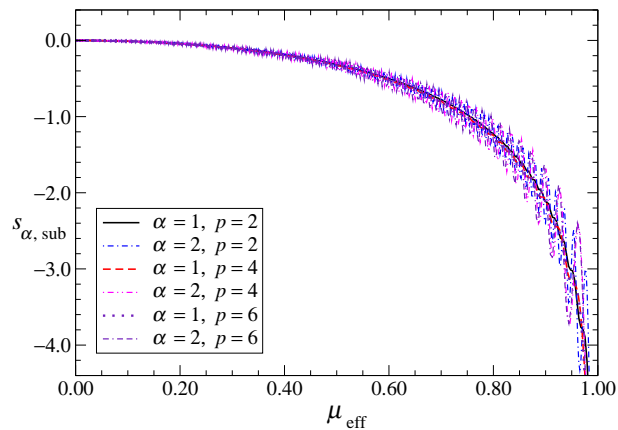


Figure 15. $s_{\alpha,sub} \equiv \frac{1}{2}[s_\alpha(x)|_{\varphi=1/2} + s_\alpha(x)|_{\varphi=3/2}] - \ln \cos \pi X$ vs. $\mu_{\text{eff}} = (x/l)^p$ for $\alpha = 1, 2$ and $p = 2, 4$ (for $l \approx 1000$) and $p = 6$ (for $l \approx 1400$).

modes should appear with length scale $\xi \sim l^\sigma$, where σ is the exponent associated with a linear external potential. The value of σ can be inferred by RG arguments analogous to those leading to the determination of the trap exponent θ at the low-density Mott transition [20], which give $\sigma = 1/3$.[‡] We thus expect that the transition region around $x = x_c$ enlarges as

$$\Delta x \sim l^{1/3}, \quad (46)$$

independently of the power-law p of the confining potential. This behaviour is confirmed by the numerical values of $\Delta x \equiv l - x_{\text{max}}$, where x_{max} is the abscissa of the rightmost maximum of $s_\alpha(x)$, interpolated to continuous x ; figure 16 shows the perfect agreement

[‡] The exponent σ can be determined by a RG analysis of the perturbation corresponding to a linear potential $V_l(x) = ux$, i.e., $\int d^d x dt V_l(x) |\phi(x, t)|^2$, at the fixed point of the continuous theory describing the Mott transition [19]. The exponent σ is related to the RG dimension y_u of the parameter u , which can be obtained from the relations $y_u - 1 = d + z - y_{|\phi|^2} = y_\mu = 2$, thus $y_u = 3$, and therefore $\sigma \equiv 1/y_u = 1/3$ for $d = 1$ and $d = 2$.

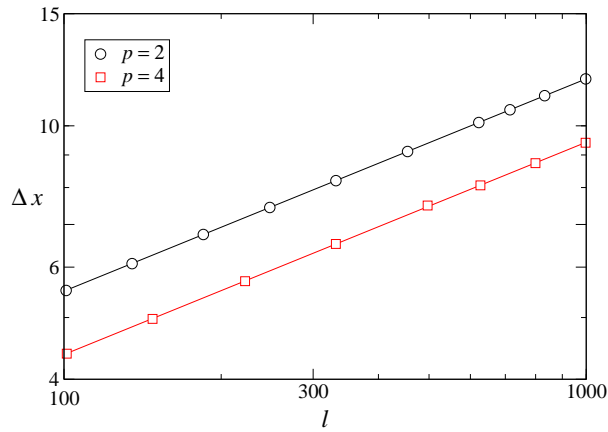


Figure 16. Δx vs. l for $\alpha = 2$, $p = 2, 4$ and $\varphi = 1/2$. The solid lines are one-parameter fits with the form $al^{1/3}$, cf. (46).

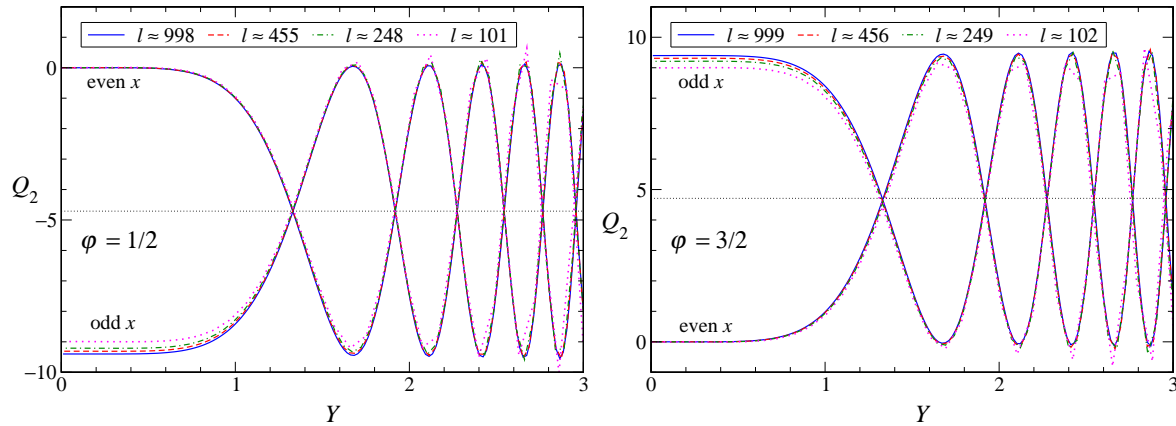


Figure 17. The function $Q_2(x)$, cf. (47), vs. $Y \equiv xl^{-2/3}$, for $p = 2$ and $\varphi = 1/2, 3/2$.

with (46).

The behaviours of the subleading and oscillating $O(\xi^{-1/\alpha})$ corrections are instead more subtle. In order to study them, we consider the function

$$Q_\alpha(x) = \xi_e^{1/\alpha} [s_\alpha(x) - s_1(x)] \quad (47)$$

for $\alpha > 1$. Assuming that the leading behaviour is given by the same function $f(X)$ for any α , Q_α should provide the $O(\xi_e^{-1/\alpha})$ term in (43). The functions $Q_\alpha(x)$ for $\alpha = 2, 3$, $p = 2, 4$, and $\varphi = 1/2, 3/2$ are shown in figures 17, 18 and 19, as obtained by numerical results at fixed trap size for $10^2 \lesssim l \lesssim 10^3$. They clearly show the expected even-odd spatial effect proportional to $(-1)^x = e^{2ik_F x}$, but also a φ -dependent scaling limit as a function of $Y = x/l^\zeta$ with $\zeta = p/(p+1)$. More precisely, the numerical results show that the asymptotic behaviour of the the functions $Q_\alpha(x)$ can be written as

$$Q_\alpha(x) \approx (-1)^x g_{\alpha,o}(Y, \varphi) + g_{\alpha,s}(Y, \varphi) \quad (48)$$

apart from further suppressed scaling corrections. Note that this strong evidence of scaling provides also an indirect and accurate check of the initial hypothesis that the

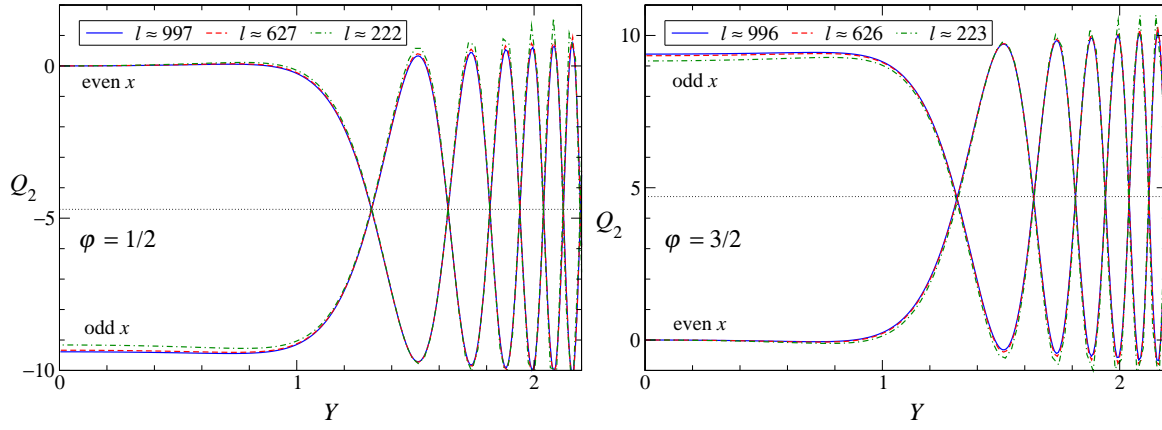


Figure 18. The function $Q_2(x)$, cf. (47), vs. $Y \equiv xl^{-4/5}$, for $p = 4$ and $\varphi = 1/2, 3/2$.

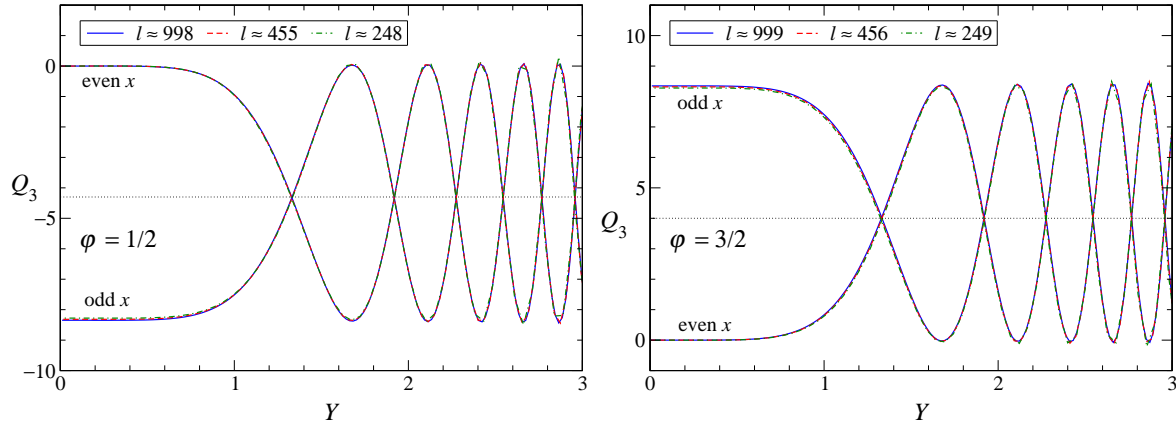


Figure 19. The function $Q_3(x)$, cf. (47), vs. $Y \equiv xl^{-2/3}$, for $p = 2$ and $\varphi = 1/2, 3/2$.

leading behaviour as a function of X does not depend on α , as in the $p \rightarrow \infty$ limit. Summarizing, we have

$$s_\alpha(x) = f(X) + \xi_e^{-1/\alpha} [(-1)^x g_{\alpha,o}(Y, \varphi) + g_{\alpha,s}(Y, \varphi)] + O(\xi_e^{-2/\alpha}) \quad (49)$$

where $X \equiv x/\xi_e$ and $Y \equiv x/l^\zeta$. We note that the behaviour of the von Neumann entropy, $\alpha \rightarrow 1$, is quite similar to that of the particle density, which turns out to be [22]

$$\langle n_x \rangle \approx \rho_{\text{lda}}(X) + \xi_e^{-1} [(-1)^x h_o(Y, \varphi) + h_s(Y, \varphi)] \quad (50)$$

Moreover, as shown by figures 20 and 21, for $p = 2$ and $p = 4$ respectively, the oscillations appear to be very close to periodic functions when plotted versus Y^{p+1} . This is particularly verified in the case of the harmonic potential, where the data at the odd and even peaks of the gap, corresponding to ground states with odd and even particle number N , accurately fit the simple function

$$Q_\alpha(x)|_{\varphi=1/2, 3/2} \approx (-1)^N b_\alpha [(-1)^x \cos(cY^3) - 1] \quad (51)$$

where b_α are the same constants entering the behaviour of the Rényi entropies of the homogeneous system, and $c \approx 2/3$. In figure 22 we show data for other values of φ .

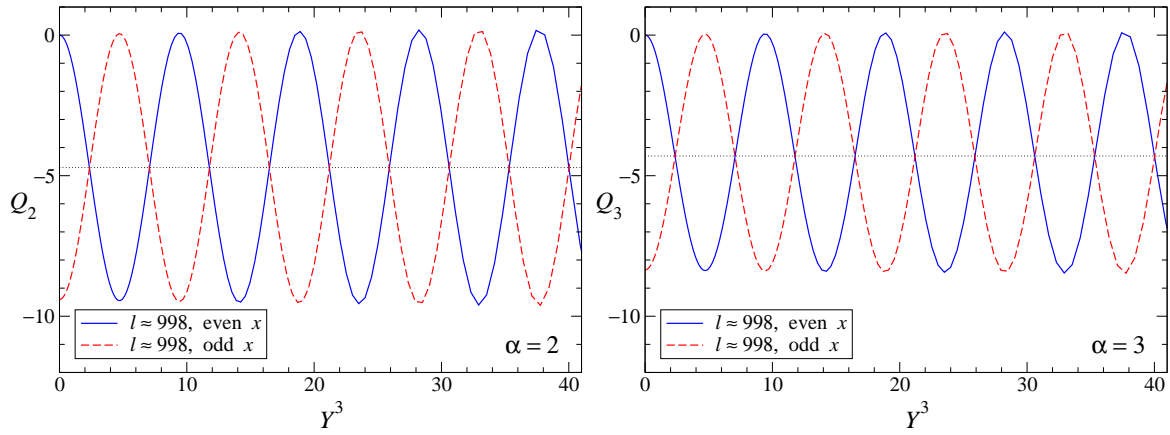


Figure 20. The functions $Q_\alpha(x)$, cf. (47), vs. $Y^3 \equiv x^3/l^2$, for $p = 2$, $\varphi = 1/2$, and $\alpha = 2, 3$.

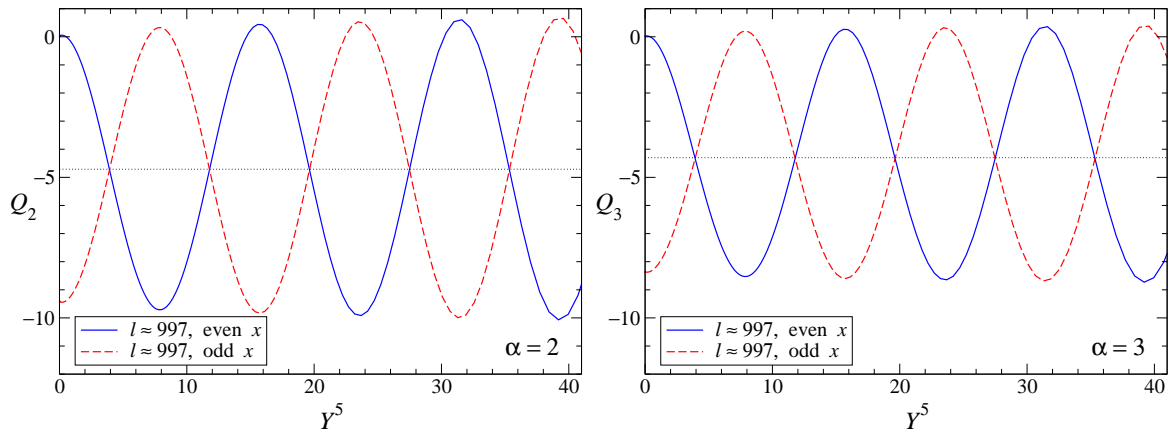


Figure 21. The functions $Q_\alpha(x)$, cf. (47), vs. $Y^5 \equiv x^5/l^4$, for $p = 4$, $\varphi = 1/2$, and $\alpha = 2, 3$.

Apart from the prefactor $(-1)^N$, there is a small residual dependence on φ , which is apparently relegated to a small dependence of c on φ .

4. Conclusions

In this paper we have investigated the scaling behaviour of the bipartite entanglement of 1D lattice systems in the presence of a power-law confining potential $V(r) = (r/l)^p$, at a quantum critical point. We have considered lattice systems whose quantum critical behaviours are described by 2D conformal field theories in the absence of the trap, thus showing logarithmically divergent entanglement entropies, see, e.g., (11).

We have considered 1D lattice models of even size L and open boundary conditions, with a trap of size l centered between the middle sites of the chain. We have divided the chain in two parts of length $l_A \equiv L/2 - x$ and $L - l_A$, and computed their von Neumann and Rényi entropies $S_\alpha(L/2 - x; L)$. In the presence of a trap of size l , the dependence on L disappears when $L \rightarrow \infty$, leaving only the dependence on x and the trap size l . We have studied the scaling behaviour of the bipartite entanglement with increasing the

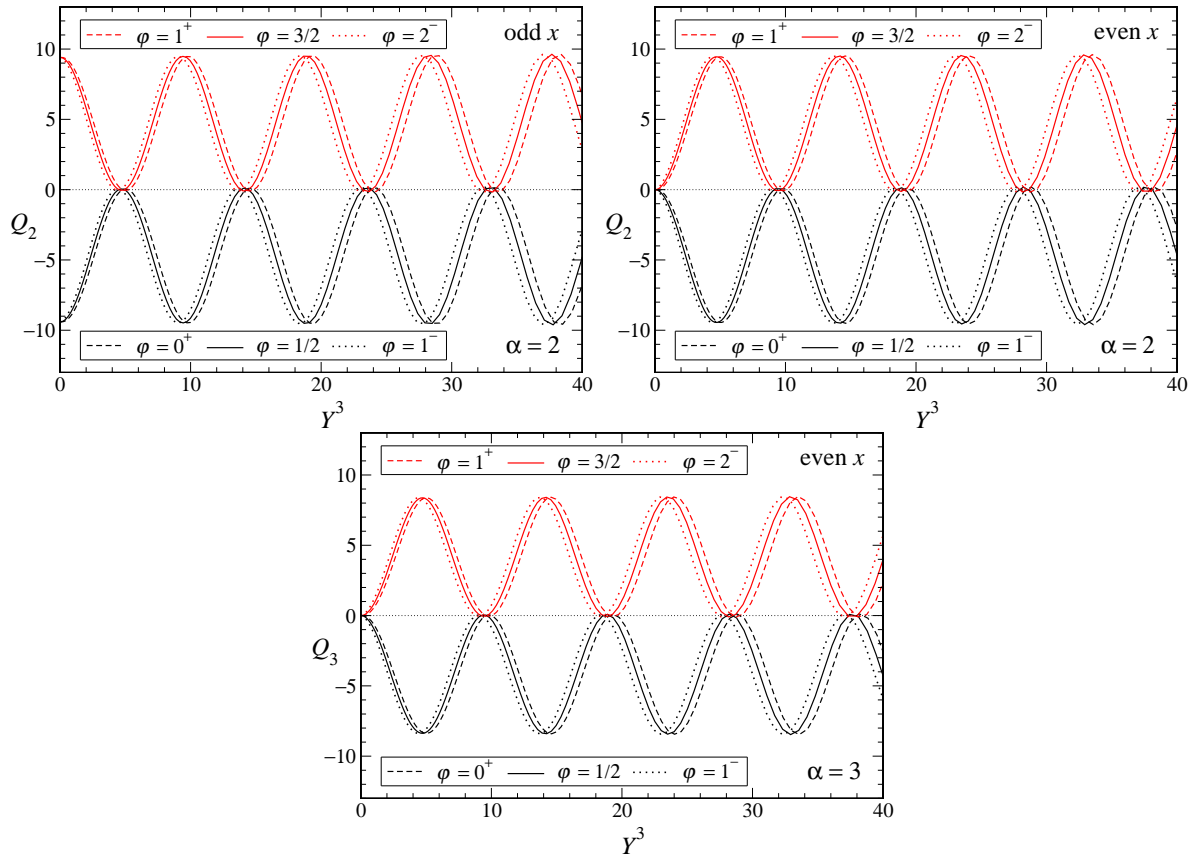


Figure 22. The functions $Q_\alpha(x)$, cf. (47), vs. $Y^3 \equiv x^3/l^2$, for $p = 2$, $\alpha = 2, 3$, several values of φ , for sites with even and odd parity, and trap sizes $l \approx 998$. Q_α as a function of φ has jumps for integer φ ; we denote $\lim_{\varphi \searrow n}$ by $\varphi = n^+$ and $\lim_{\varphi \nearrow n}$ by $\varphi = n^-$.

trap size, keeping the other model parameters fixed at the quantum critical point of the homogeneous system without trap.

As a theoretical laboratory, we have considered the quantum XY chain in an external space-dependent transverse field, acting as a trap for the spinless fermions of its quadratic Hamiltonian representation. This model presents a quantum critical transition belonging to the 2D Ising universality class, thus described by a CFT with central charge $c = 1/2$. In the presence of the trap and for large trap sizes, the quantum critical behaviour can be described in the framework of the TSS theory [20], where the quantum critical behaviour is cast in the form a TSS, cf. (7), with a nontrivial trap exponent $\theta = p/(p+1)$, which determines how the length scale of the critical modes at the critical point diverges with increasing trap size, i.e., $\xi \sim l^\theta$. Exploiting the quadratic spinless fermion representation of the XY chain, we have computed the bipartite von Neumann and Rényi entanglement entropies up to $l \approx 10^4$. Our results show that at the quantum critical point they behave as

$$\lim_{L \rightarrow \infty} S_\alpha(L/2 - x; L) = C_\alpha \left[\ln \xi_1 + \ln R_\alpha + e_\alpha + f_\alpha(X) + O(\xi_1^{-1/\alpha}) \right], \quad (52)$$

$$\xi_1 = a_1 \gamma^{\theta/p} l^\theta [1 + O(l^{-\theta})], \quad X \equiv x/\xi_1, \quad \xi_\alpha/\xi_1 = R_\alpha + O(\xi_1^{-1/\alpha}),$$

where $C_\alpha = c(1 + \alpha^{-1})/12$, $c = 1/2$ is the central charge, and e_α is the same constant entering the entanglement entropies of homogeneous systems with open boundary conditions, cf. (13). The entanglement length scales ξ_α are defined by imposing $S_\alpha(L/2; L) \equiv C_\alpha(\ln \xi_\alpha + e_\alpha)$; the length scales ξ_α , and in particular ξ_1 derived from the von Neumann entropy, behave consistently with the predictions of the TSS theory, with $\theta = p/(p+1)$ and a_1 independent of γ . The asymptotic ratios R_α and the functions $f_\alpha(X)$ depend on the power of the potential, show a small dependence on α , but are universal with respect to the parameter γ , see figures 4, 6, and 7. Moreover, in the $p \rightarrow \infty$ limit they tend to $f_\alpha(X) = \ln \cos \pi X$ with $X = x/L$, which is the behaviour in the homogeneous system with open boundary conditions.

We have studied the scaling of the entanglement of confined particle systems described by the 1D BH model (1) in the presence of a power-law confining potential, with the center of the trap in the superfluid phase. This model is of experimental relevance because it describes cold atoms in quasi-one-dimensional optical lattices. We have computed bipartite entanglement in the hard-core limit of the model, which allows very accurate numerical calculations by exploiting a map into a lattice model of free spinless fermions. In the absence of the trap, the continuum theory corresponding to the gapless superfluid phase is a 2D massless boson field theory, thus a CFT with $c = 1$. In this region the trap-size dependence presents new features with respect to the XY chain: a multiscaling behaviour with the existence of different length scales which diverge with distinct power laws in the TSS; the presence of level crossings of the lowest states at finite trap size, which gives rise to periodic modulations of the amplitudes of the asymptotic power-law behaviours, with a period given by the asymptotically constant interval between the level crossings. We have shown that the bipartite entanglement entropy presents the same features as well. We have computed the von Neumann and Rényi entropies at $\mu = 0$ corresponding to half filling $f = 1/2$ in the absence of the trap, up to trap sizes $l \approx 10^3$, corresponding to total particle numbers $N = O(10^3)$. Our results provide a robust numerical evidence of the following scaling behaviour

$$\begin{aligned} \lim_{L \rightarrow \infty} S_\alpha(L/2 - x; L) &= C_\alpha \left\{ \ln \xi_e + e_\alpha + f(X) \right. \\ &\quad \left. + \xi_e^{-1/\alpha} [(-1)^x g_{\alpha,o}(Y, \varphi) + g_{\alpha,s}(Y, \varphi)] + O(\xi_e^{-2/\alpha}) \right\}, \\ \xi_e &= a_e l, \quad X \equiv x/\xi_e, \quad Y \equiv x/l^{p/(p+1)}, \end{aligned} \quad (53)$$

where e_α and a_e are constant given in equations (35) and (38) respectively. The leading spatial dependence $f(X)$ turns out to be independent of α ; it depends on p , approaching the CFT dependence $f(X) = \ln \cos(\pi X)$ with $X = x/L$ when increasing p , which is the result holding in a homogeneous chain of size L . The $O(\xi_e^{-1/\alpha})$ term presents an even-odd spatial effect proportional to $(-1)^x = e^{2ik_F x}$, scaling as a function of $Y = x/l^\zeta$ with $\zeta = p/(p+1)$, modulated by the variable φ defined in equation (31), see figures 17, 18, 19. For the harmonic potential, an accurate description of $O(\xi_e^{-1/\alpha})$ term is given by $(-1)^N b_\alpha [(-1)^x \cos(cY^3) - 1]$, see figure 20.

The above scaling behaviours have been mostly obtained by analyzing the scaling of

numerical (practically exact) results at finite trap size. Of course, it would be worthwhile to derive analytically the asymptotic trap-size dependence of the entanglement entropy, which may lead to further physical insights.

Acknowledgments

Helpful discussions with Pasquale Calabrese are gratefully acknowledged.

References

- [1] Calabrese P, Cardy J and Doyon B Eds. 2009 *Entanglement entropy in extended quantum systems*, *J. Phys. A: Math. Theor.* **42** 500301
- [2] Holzhey C, Laursen F and Wilczek F 1994 *Nucl. Phys. B* **424** 443
- [3] Vidal G, Latorre J I, Rico E and Kitaev A 2003 *Phys. Rev. Lett.* **90** 227902
- [4] Calabrese P and Cardy J 2004 *J. Stat. Mech.* P06002
- [5] Calabrese P and Cardy J 2009 *J. Phys. A: Math. Theor.* **42** 504005
- [6] Bloch I, Dalibard J and Zwirger W 2008 *Rev. Mod. Phys.* **80** 885
- [7] Greiner M, Bloch I, Mandell M O, Hänsch T and Esslinger T 2002 *Nature* **415** 39
- [8] Stöferle T, Moritz H, Schori C, Köhl M and Esslinger T 2004 *Phys. Rev. Lett.* **92** 130403
- [9] Paredes B, Widera A, Murg V, Mandel O, Fölling S, Cirac I, Shlyapnikov G, Hänsch R W and Bloch I 2004 *Nature* **429** 277
- [10] Kinoshita T, Wenger T and Weiss D S 2004 *Science* **305**, 1125
- [11] Kinoshita T, Wenger T and Weiss D S 2005 *Phys. Rev. Lett.* **95** 190406
- [12] Hadzibabic Z, Krüger P, Cheneau M, Battelier B and Dalibard J 2006 *Nature* **441** 1118
- [13] Krüger P, Hadzibabic Z and Dalibard J 2007 *Phys. Rev. Lett.* **99** 040402
- [14] Fölling S, Widera A, Müller T, Gerbier F and Bloch I 2006 *Phys. Rev. Lett.* **97** 060403
- [15] Spielman I B, Phillips W D and Porto J V 2007 *Phys. Rev. Lett.* **98** 080404
- [16] Spielman I B, Phillips W D and Porto J V 2008 *Phys. Rev. Lett.* **100** 120402
- [17] Clément D, Fabbri N, Fallani L, Fort C and Inguscio M 2009 *Phys. Rev. Lett.* **102** 155301
- [18] Jaksch D, Bruder C, Cirac J I, Gardiner C W and Zoller P 1998 *Phys. Rev. Lett.* **81** 3108
- [19] Fisher M P A, Weichmann P B, Grinstein G and Fisher D S 1989 *Phys. Rev. B* **40** 546
- [20] Campostrini M and Vicari E 2010 *Phys. Rev. A* **81** 023606
- [21] Campostrini M and Vicari E 2009 *Phys. Rev. Lett.* **102** 240601
- [22] Campostrini M and Vicari E 2010 *Phys. Rev. A* **81** 063614
- [23] Calabrese P and Lefevre A 2008 *Phys. Rev. A* **78** 032329
- [24] Peschel I 2003 *J. Phys. A: Math. Gen.* **36** L205
- [25] Latorre J I and Riera A 2009 *J. Phys. A: Math. Theor.* **42** 504002
- [26] Eisler V, Iglói F and Peschel I 2009 *J. Stat. Mech.* P02011
- [27] Sachdev S 1999 *Quantum Phase Transitions* (Cambridge Univ. Press)
- [28] Jin B-Q and Korepin V E 2004 *J. Stat. Phys.* **116** 79
- [29] Iglói F and Juhász R 2008 *Europhys. Lett.* **81** 57003
- [30] Calabrese P and Cardy J 2010 *J. Stat. Mech.* P04023
- [31] Calabrese P, Campostrini M, Essler F and Nienhuis B 2010 *Phys. Rev. Lett.* **104** 095701
- [32] Lafflorencie N, Sorensen E S, Chang M-S and Affleck I 2006 *Phys. Rev. Lett.* **96** 100603
- [33] Zhou H-Q, Barthel T, Fiaerestad J and Schollwöck U 2006 *Phys. Rev. A* **74** 050305